

# We are IntechOpen, the world's leading publisher of Open Access books Built by scientists, for scientists

**4,800**

Open access books available

**122,000**

International authors and editors

**135M**

Downloads

Our authors are among the

**154**

Countries delivered to

**TOP 1%**

most cited scientists

**12.2%**

Contributors from top 500 universities



**WEB OF SCIENCE™**

Selection of our books indexed in the Book Citation Index  
in Web of Science™ Core Collection (BKCI)

Interested in publishing with us?  
Contact [book.department@intechopen.com](mailto:book.department@intechopen.com)

Numbers displayed above are based on latest data collected.

For more information visit [www.intechopen.com](http://www.intechopen.com)



# The Application of Inorganic Nanomaterials in Dye-Sensitized Solar Cells

Zhigang Chen, Qiwei Tian, Minghua Tang and Junqing Hu  
*State Key Laboratory for Modification of Chemical Fibers and Polymer Materials,  
College of Materials Science and Engineering, Donghua University  
China*

## 1. Introduction

Energy crisis and environment pollution cause a great quest and need for environmentally sustainable energy technologies. Among all the renewable energy technologies, photovoltaic technology utilizing solar cell has been considered as the most promising one (Chen et al., 2007a; Gratzel, 2001). As early as in 1954, researchers demonstrated the first practical conversion from solar radiation to electricity by a *p-n* junction type solar cell with 6% efficiency (Chapin et al., 1954). Up to now, the common solar power conversion efficiencies of this type solar cell are beyond 15% (Tributsch, 2004). Unfortunately, the relatively high cost of manufacturing and the use of toxic chemicals have prevented their widespread use, which prompts the search for high efficient, low cost and environmentally friendly solar cells.

Semiconductor with a very large bandgap, such as  $\text{TiO}_2$ ,  $\text{ZnO}$  and  $\text{SnO}_2$ , can be employed to construct solar cells. But these materials can only be excited by ultraviolet or near-ultraviolet radiation that occupies only about 4% of the solar light. Dye molecules as light absorbers for energy conversion have shaped evolution via the process of photosynthesis and photo-sensoric mechanisms (Tributsch, 2004). Dye sensitization of semiconductor with a wide band-gap has provided a successful solution to extending the absorption range of the cells to long wavelength region. This approach also presents advantages over the direct band-to-band excitation in conventional solar cells, since attached dyes, rather than the semiconductor itself, are the absorbing species (Garcia et al., 2000). Importantly, light absorption and charge carrier transport are separated, and the charge separation takes place at the interface between semiconductor and sensitizer, preventing electron-hole recombination. Since the discovery of the photocurrents resulting from dye sensitization of semiconductor electrodes in 1968, dyes have been widely used in electrochemical energy converting cells (Tributsch, 1972).

During the first years of the sensitized solar cell research, most studies were made with single crystal oxide samples, because by eliminating grain boundaries and high concentrations of surface states the interpretation of the results became more transparent (Tributsch, 2004). However, at that time, the power conversion efficiencies were very low (<1%). Tsubomura *et al.* reported a breakthrough in the conversion efficiency in 1976 (Tsubomura et al., 1976). They used the powdered high porosity multi-crystalline  $\text{ZnO}$  instead of single crystal semiconductor, resulting in a significant increase of the surface area of the electrode. When the dye (Rose Bengal) was used as the sensitizer, an energy efficiency of 1.5% was obtained for light incident within the absorption spectrum of the sensitizer.

Later, in 1980, Tsubomura group increased the surface roughness of ZnO samples and demonstrated an energy efficiency of 2.5%, also for light incident within the absorption spectrum of the sensitizer (Matsumura et al., 1980).

A significant advance in the field of dye-sensitized solar cells (DSCs, also considered as Grätzel cell) was made through the efforts of Grätzel and coworkers in 1991 (Fig. 1) (Oregan & Gratzel, 1991). They greatly improved the power energy conversion efficiency from lower than 2.5 to 7%, and the main reasons for the improvement were as follows: (1) the preparation of nanostructured TiO<sub>2</sub> film (Desilvestro et al., 1985), (2) the use of ruthenium complex that was adequately bonded to TiO<sub>2</sub> nanoparticles and (3) the selected organic liquid electrolyte based on iodide/triiodide. The jump in solar energy conversion efficiency has attracted considerable attentions and motivated significant optimism with respect to the feasibility of DSCs as a cost-effective alternative to conventional solar cells.

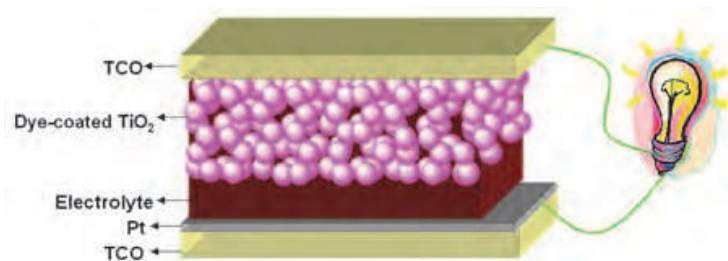


Fig. 1. Typical sandwich-type dye-sensitized TiO<sub>2</sub> nanocrystal solar cell.

The typical DSCs are composed of a transparent nanoporous semiconductor electrode on transparent conducting optically (TCO) glass, a very thin layer of light-absorbing material (dyes) – sensitizer on the entire surface of semiconductor (such as TiO<sub>2</sub>) electrode, a counter electrode (such as Pt), and a transparent hole conductor (electrolyte) filling the pores, in contact with the light-absorbing layer at all points. The typical dye-sensitized TiO<sub>2</sub> nanocrystal solar cell is shown in Fig. 1. The operational principle of DSCs is described as follows. Photons enter DSCs and can be absorbed by dye molecules (D) at various depths in the film. The dye molecule after absorbing photon will then be promoted into its excited state (D\*) from where it is now energetically able to inject an electron into the conduction band of semiconductor, leaving an oxidized dye (D<sup>+</sup>) on the semiconductor surface. The injected electrons percolate via the interconnected nanoparticles to the substrate and are fed into an electrical circuit, where it can deliver work. Subsequently, the electrons, which now carry less energy, enter the cell again via the counter electrode and transport to hole-conductor materials (commonly the organic electrolyte containing iodide/triiodide, this process can be described as:  $I_3^- + 2e^- \rightarrow 3I^-$ ). The oxidized dye (D<sup>+</sup>) is then reduced back to its original state by hole-conductor materials (such as, this process can be typically described as:  $2D^+ + 3I^- \rightarrow 2D + I_3^-$ ). Then the cycle is completed.

The main issues for the development of DSCs are to improve their photoelectric conversion efficiency, thermostability and long-term stability, which are strongly dependent on the advances in nanotechnology and nanomaterials. It is well known that nanotechnology opens a door to tailing materials and creating various nanostructures for the use in dye-sensitized solar cells. A predominant feature of these nanostructures is that the size of their basic units is on nanometer scale (10<sup>-9</sup> m), and inorganic nanomaterials therefore present an internal surface area significantly larger than that of bulk materials. Currently, inorganic nanomaterials have been widely used in all components in DSCs, including transparent

semiconductor electrode, counter electrode, electrolyte and light-absorbing material. In this chapter, the recent progress on the selection and utilization of inorganic nanomaterials in dye-sensitized solar cells are mainly introduced and discussed.

## 2. The application of semiconductor nanomaterials in photoanodes

Compared to bulk materials, semiconductor nanomaterials as photoanodes can offer a larger surface area for dye adsorption, contributing to optical absorption and leading to an improvement in the solar cell conversion efficiency. As photoelectrode materials in DSCs, the semiconductor nanostructures are usually classified into two types: (1) nanoparticles, which offer large surface area to photoanodes for dye-adsorption, however have recombination problem due to the existence of considerable grain boundaries in the film. To settle this issue, core-shell structure derived from the nanoparticles by forming a coating layer has been developed and applied to DSCs with a consideration of suppressing the interfacial charge recombination, while this kind of structure has been proved to be less effective and lack of consistency and reproducibility; (2) one-dimensional nanostructures such as nanowires and nanotubes, which are advantageous in providing direct pathways for electron transport much faster than in the nanoparticle film, however face drawback of insufficient internal surface area of the photoelectrode film, leading to relatively low conversion efficiency (Zhang & Cao, 2011). This section aims to demonstrate semiconductor nanomaterials as photoanodes, including nanoparticles, nanowires and nanotubes.

### 2.1 Semiconductor nanoparticles

Among different nanostructures, nanoparticles have been most widely studied for the use in DSCs to form photoelectrode film (Oregan & Gratzel, 1991). This is because, to a large extent, the photoelectrode films comprised of nanoparticles can give a high specific surface area, resulting in an efficient extinction of incident light within film which is a few microns thick. And the anodes of DSCs are typically constructed with the nanoparticles film (thickness:  $\sim 10 \mu\text{m}$ ) of wide bandgap semiconductor including  $\text{SnO}_2$ ,  $\text{ZnO}$ , and  $\text{TiO}_2$ .

Among these wide bandgap semiconductors, titania ( $\text{TiO}_2$ ), an n-type semiconductor with a wide bandgap (3.2 eV for anatase), has been well known and widely used in the photoanode of DSCs. As early as 1985, Desilvestro et al (Desilvestro et al., 1985) have showed that if  $\text{TiO}_2$  is used in a nanoparticle form, the power conversion efficiency of DSC can be drastically enhanced. The improvement of conversion efficiency lies in the superiority of nanoparticles to create large surface, which was demonstrated by a comparison between a flat film and a 10- $\mu\text{m}$ -thick film that consisted of nanoparticles with an average size of 15 nm (Oregan & Gratzel, 1991). The latter, nanoparticle film, showed a porosity of 50-65% and gave rise to almost 2000-fold increase in the surface area. Fig. 2 shows typical cross-section morphology of  $\text{TiO}_2$  nanoparticle film with thickness of about 4  $\mu\text{m}$ .

For state-of-the-art DSCs, the employed architecture of the mesoporous  $\text{TiO}_2$  electrode is as follows (Hagfeldt et al., 2010): (a) a  $\text{TiO}_2$  blocking layer (thickness  $\sim 50 \text{ nm}$ ), coating TCO glass to prevent contact between the redox mediator in the electrolyte and TCO glass; (b) a light absorption layer consisting of a  $\sim 10 \mu\text{m}$  thick film of mesoporous  $\text{TiO}_2$  with  $\sim 20 \text{ nm}$  particle size that provides a large surface area for sensitizer adsorption and good electron transport to the substrate; (c) a light scattering layer on the top of the mesoporous film, consisting of a  $\sim 3 \mu\text{m}$  porous layer containing  $\sim 400 \text{ nm}$  sized  $\text{TiO}_2$  particles; (d) an ultrathin overcoating of  $\text{TiO}_2$  on the whole structure, deposited by means of chemical bath deposition (using aqueous  $\text{TiCl}_4$  solution), followed by heat treatment.

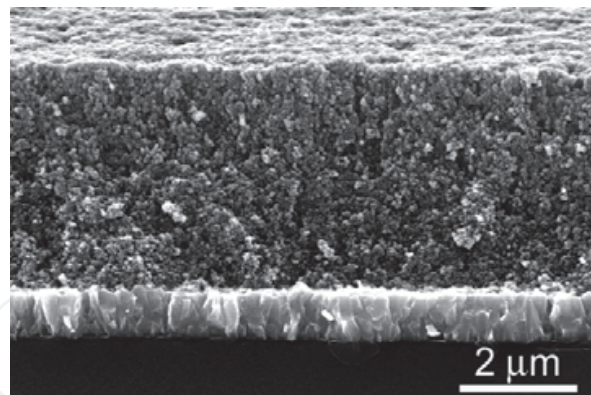


Fig. 2. Cross-section morphology of typical TiO<sub>2</sub> nanoparticle film.

Furthermore, it has mentioned that the performance of solar cell is intimately linked to the structure and morphology of the nanoporous oxide layer. For efficient dye distribution, the surface area of the membrane film must be large and porous. So the preparation procedure of TiO<sub>2</sub> nanoparticle film must be optimized so as to provide an optimal particle size and porosity features. Up to now, the main synthesis methods of TiO<sub>2</sub> nanoparticle film for DSCs include sol-gel/hydrothermal synthesis (Muniz et al., 2011), electrochemical deposition (Murakami et al., 2004), magnetron sputtering (Sung & Kim, 2007), chemical vapor deposition (Murakami et al., 2004) and so on.

The most common technique for the preparation of TiO<sub>2</sub> nanoparticles is sol-gel/hydrothermal synthesis, which involves the hydrolysis of a titanium precursor such as titanium (IV) alkoxide with excess water catalyzed by acid or base, followed by hydrothermal growth and crystallization. Acid or basic hydrolysis gives materials of different shapes and properties; while the rate of hydrolysis, temperature, and water content can be tuned to produce particles with different sizes. Transmission electron microscopy measurements revealed that for TiO<sub>2</sub> nanoparticles prepared under acidic conditions, crystalline anatase particles were formed exposing mainly the <101> surface (Zaban et al., 2000). Compared with nitric acid, employing acetic acid increases the proportion of the <101> face about 3-fold (Zaban et al., 2000). The differences can be explained by different growth rates: in acetic acid crystal growth is enhanced in the <001> direction compared with the growth in the presence of nitric acid (Neale & Frank, 2007). Hore et al. (Hore et al., 2005) found that base-catalyzed conditions led to mesoporous TiO<sub>2</sub> that gave slower recombination in DSCs and higher *V*<sub>oc</sub> but a reduced dye adsorption compared with the acid-catalyzed TiO<sub>2</sub>. The produced TiO<sub>2</sub> nanoparticles are formulated in a paste with polymer additives and deposited onto TCO glass using screen printing techniques. Finally, the film is sintered at about 450 °C in air to remove organic components and to make electrical connection between the nanoparticles.

It has been found that pure TiO<sub>2</sub> nanoparticles are not perfect in terms of solar cell efficiency, since the charge recombination between the injected electrons in conductor band of TiO<sub>2</sub> and electron acceptors in the electrolyte is unavoidable to diminish both photovoltage and photocurrent, thus limiting the device efficiency (Gregg et al., 2001). To improve device efficiency, one effective approach is to grow a thin coating layer of another oxide on the surface of TiO<sub>2</sub> particles. Thus, coating TiO<sub>2</sub> nanoparticles with a different metal oxide to build core-shell structure has received much attention (Kay & Gratzel, 2002). Now, two approaches have been developed to create such core-shell structure (Zhang & Cao, 2011). One involves a first synthesis of nanoparticles and then fabricating a shell layer

on the surface of nanoparticles. This leads to the formation of core-shell structured nanoparticles, with which the film photoanode is prepared then. Such an approach builds up a photoelectrode structure as shown in Fig. 3a, and an energy barrier is formed at the interfaces not only between nanoparticle/electrolyte but also between the individual core nanoparticles. In another approach, the nanoparticle film photoanode is prepared prior to the deposition of shell layer, receiving a structure as shown in Fig. 3b. The latter approach is obviously advantageous in electron transport that happens within single material, but there is usually a challenge in the fabrication of shell layer regarding a complete penetration and ideal coating of the shell material. Metal oxides such as ZnO, CaCO<sub>3</sub>, Nb<sub>2</sub>O<sub>3</sub>, SrTiO<sub>3</sub>, MgO and Al<sub>2</sub>O<sub>3</sub> have been usually used as the coating layer for TiO<sub>2</sub>. Table 1 shows photoelectric conversion efficiencies of DSCs based on TiO<sub>2</sub> and metal oxides-coated TiO<sub>2</sub> electrodes, which demonstrates the improved efficiency of DSCs employing a core-shell structured TiO<sub>2</sub> electrode. This improvement should be attributed to the following two factors (Jung et al., 2005): First, the wide bandgap coating layer retards the back transfer of electrons to the electrolyte solution and minimizes electron-hole recombination. Second, the coating layer enhances the dye adsorption and increases the volume of the optically active component, leading to the improved cell performance. If pH of the coating oxides is more basic than that of TiO<sub>2</sub>, the carboxyl groups in a dye molecule are more easily adsorbed to their surface.

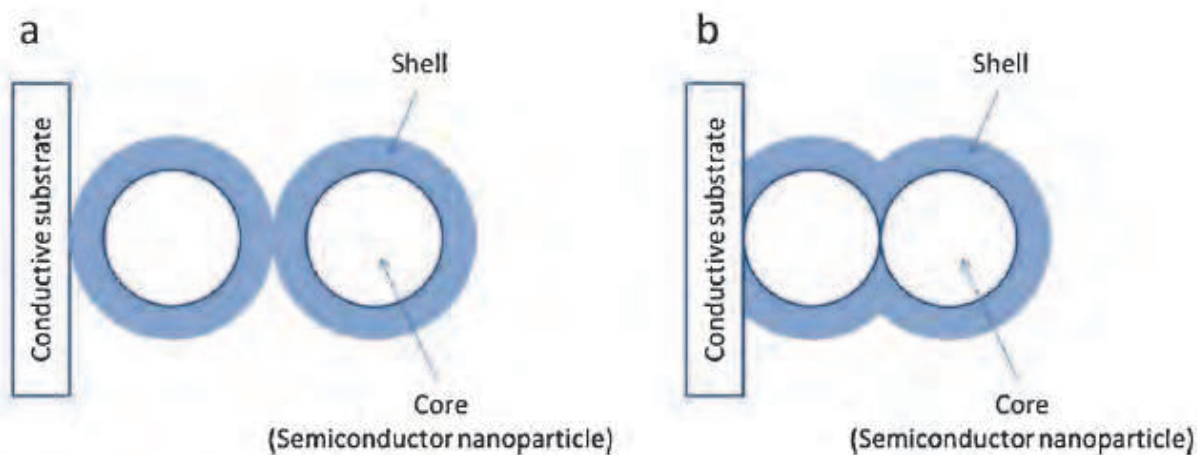


Fig. 3. Core-shell structures used in DSCs. (a) The shell layer is formed prior to the film deposition, (b) the shell layer is coated after the film deposition (Zhang & Cao, 2011).

metal oxides	ZnO	CaCO <sub>3</sub>	Nb <sub>2</sub> O <sub>3</sub>	SrTiO <sub>3</sub>	MgO	Al <sub>2</sub> O <sub>3</sub>
$\eta^b$ (%)	7.7	6.9	3.6	3.81	3.1	3.93
$\eta^c$ (%)	9.8	7.9	5.0	4.39	4.5	5.91
Ref.	(Wang et al., 2001)	(Wang et al., 2006)	(Chen et al., 2001)	(Diamant et al., 2003)	(Jung et al., 2005)	(Wu et al., 2008)

$\eta^b$  : Conversion efficiency of DSC based on the bare TiO<sub>2</sub> film

$\eta^c$  : Conversion efficiency of DSC based on the metal oxides-coated TiO<sub>2</sub> film

Table 1. Photoelectric conversion efficiency of DSCs based on TiO<sub>2</sub> and metal oxides-coated TiO<sub>2</sub> electrodes.

## 2.2 Semiconductor nanowires

Nanoparticle films have been regarded as a paradigm of porous photoanodes. However, the nanoparticle films are not thought to be ideal in structure with regard to electron transport. While one-dimensional nanostructures, such as nanowires, are advantageous in providing direct pathways for electron transport much faster and therefore giving electron diffusion length larger than in the nanoparticle films. Hence, semiconductor nanowires become a kind of promising candidate for making up the drawbacks of nanoparticle films.

### 2.2.1 TiO<sub>2</sub> nanowires

Oriented single-crystalline TiO<sub>2</sub> nanowires are an important one-dimensional nanostructure that has also attracted a lot of interests regarding an application in DSCs (Liu & Aydil, 2009). Hydrothermal growth has been reported to be a novel method for the synthesis of TiO<sub>2</sub> nanowire array on TCO glass substrate. In this method, tetrabutyl titanate and/or titanium tetrachloride are used as the precursor, to which an HCl solution is added to stabilize and control the pH of the reaction solution.

Liu et al. (Liu & Aydil, 2009) developed a facile hydrothermal method to grow oriented, single-crystalline rutile TiO<sub>2</sub> nanorod films on TCO glass substrate, as shown in Fig. 4a. The diameter, length, and density of the nanorods could be varied by changing the growth parameters, such as growth time, temperature, initial reactant concentration, acidity, and additives. The epitaxial relation between TCO glass and rutile TiO<sub>2</sub> with a small lattice mismatch played a key role in driving the nucleation and growth of the rutile TiO<sub>2</sub> nanorods. With TiCl<sub>4</sub>-treatment, DSC based on 4 μm-long TiO<sub>2</sub> nanorod film exhibited a power conversion efficiency of 3%. Furthermore, Feng et al. (Feng et al., 2008) presented a straightforward hydrothermal method to prepare single crystal rutile TiO<sub>2</sub> nanowire arrays up to 5 μm long on TCO glass via a non-polar solvent/hydrophilic substrate interfacial reaction (Fig. 4b). The as-prepared densely packed nanowires grew vertically oriented from TCO glass along the (110) crystal plane with a preferred (001) orientation (Fig. 4c). The Cl<sup>-</sup> ions were explained to play an important role in the growth of TiO<sub>2</sub> nanowires by attaching on the (110) plane of TiO<sub>2</sub> nanocrystal and thus suppressing the growth of this plane. DSCs based on 2-3 μm long nanowire array demonstrated a very encouraging power conversion efficiency of 5.02%.

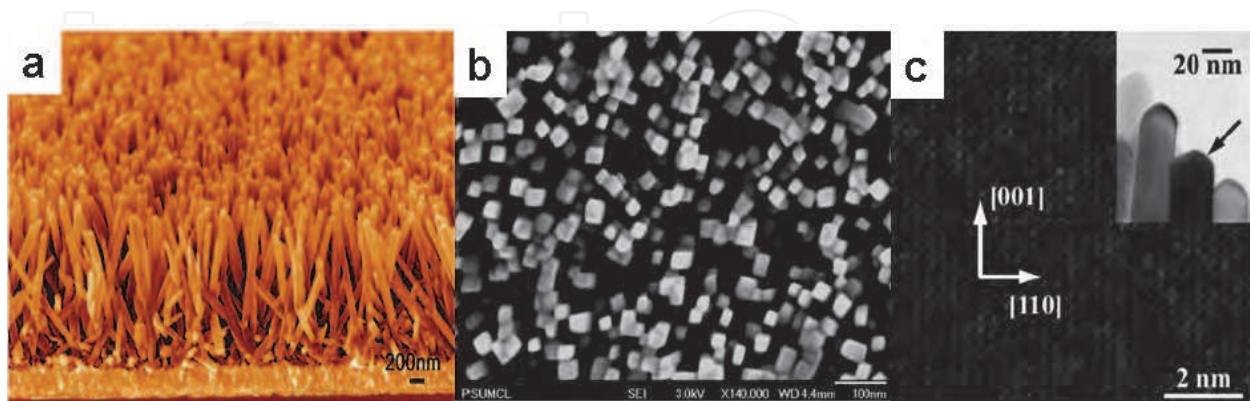


Fig. 4. DSCs with TiO<sub>2</sub> nanowires: (a) Cross sectional view of oriented rutile TiO<sub>2</sub> nanorod film grown on TCO substrate (Liu & Aydil, 2009); (b) top-view images of vertically oriented self-organized TiO<sub>2</sub> nanowire array grown on FTO coated glass (Feng et al., 2008); (c) TEM image illustrating the [001] orientation of TiO<sub>2</sub> nanowires (Feng et al., 2008).

In addition, Park et al. (Park et al., 2000) compared the performance between  $\text{TiO}_2$  nanowires and nanoparticles which were both rutile phase. The efficiency achieved by  $\text{TiO}_2$  nanowire film in 2-3  $\mu\text{m}$  thick was higher than that obtained for the nanoparticle film in 5  $\mu\text{m}$  thick. This is good evidence that the one-dimensional nanostructures may offer better charge transport than the nanoparticles. A further increase in the conversion efficiency most likely relies on the development of new fabrication techniques that can achieve longer  $\text{TiO}_2$  nanowires.

### 2.2.2 ZnO nanowires

Zinc oxide (ZnO) has remarkable optical properties with a wide bandgap (3.2 eV) and a large exciton binding energy (60 meV). In 2005, Law et al. (Law et al., 2005) reported the preparation of ZnO nanowire array on TCO glass by seed mediated liquid phase synthesis method. The experiment was purposely designed to grow ZnO nanowires with a high aspect ratio so as to attain a nanowire film with high density and sufficient surface area (Fig. 5a and b). A  $\sim 25\text{-}\mu\text{m}$ -thick film consisting of ZnO nanowires in diameter of  $\sim 130\text{ nm}$  was mentioned to be able to achieve a surface area up to one-fifth as large as a nanoparticle film used in the conventional DSCs. The superiority of ZnO nanowires for DSC application was firstly demonstrated by their high electron diffusion coefficient,  $0.05\text{-}0.5\text{ cm}^2\text{ s}^{-1}$ , which is several hundred times larger than that of nanoparticle films. Larger diffusion coefficient means longer diffusion length. In other words, the photoanode made of nanowires allows for thickness larger than that in the case of nanoparticles. This can compensate for the insufficiency of surface area of the nanowire-based photoanode. DSC based on ZnO nanowire gave a power conversion efficiency of 1.5%. In the same year, Prof. Aydil group also successfully prepared ZnO nanowire array on TCO glass and then fabricated a DSC with a conversion efficiency of 0.5% (Baxter & Aydil, 2005).

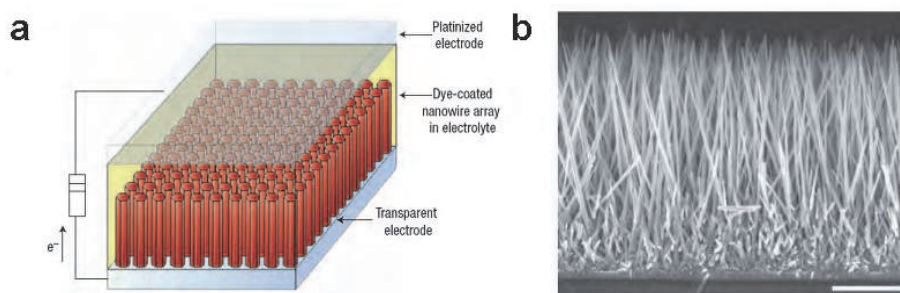


Fig. 5. Nanowire dye-sensitized cell based on ZnO wire array. (a) Schematic diagram of the cell; (b) Typical scanning electron microscopy cross-section of a cleaved nanowire array on TCO Scale bar= $5\text{ }\mu\text{m}$ . (Law et al., 2005).

## 2.3 Semiconductor nanotubes

Nanotubes are a class of very important one-dimensional nanostructure since their hollow structure may usually give surface area larger than that of nanowires or nanorods. The nanotube arrays are ordered and strongly interconnected, which eliminates randomization of the grain network and increases contact points for good electrical connection.

### 2.3.1 $\text{TiO}_2$ nanotubes

$\text{TiO}_2$  nanotubes have been prepared by several methods including anodization, sol-gel, and hydrothermal synthesis and so on. Among these methods, anodization of titanium metal



has been an intensively employed method for the fabrication of the oriented TiO<sub>2</sub> nanotube array which could combine high surface area with well-defined pore geometry (Zhu et al., 2007). The vertical pore geometry of the nanotubes appears to be more suitable than the conventional random pore network for the fabrication of DSCs, especially DSCs with quasi-solid/solid-state electrolytes. It has been also reported that nanotube arrays give enhanced light scattering and improved collection efficiencies compared to conventional sol-gel-derived TiO<sub>2</sub> films with the same thickness (Zhu et al., 2007).

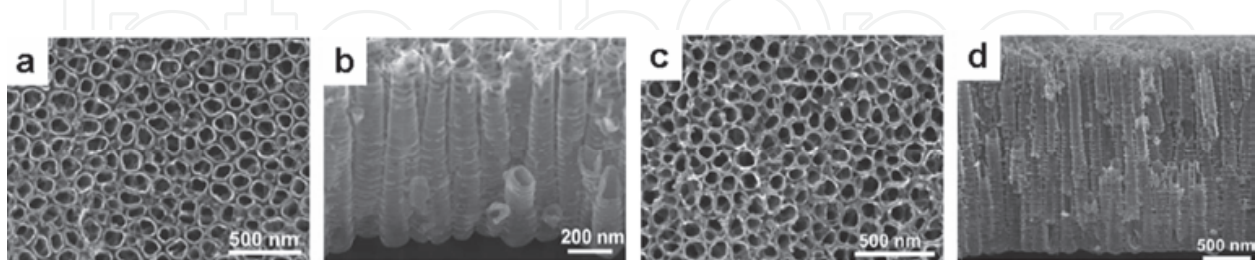


Fig. 6. SEM top-views (a, c) and cross-sections (b, d) for the “short” and “long” tubes (Macak et al., 2005).

By anodization of Ti metal in fluoride-based electrolytes, TiO<sub>2</sub> nanotubes can be prepared from Ti foil, but nanotube growth can also be obtained from Ti thin film deposited on TCO glass. The length of the nanotubes, wall thickness, pore diameter, and tube-to-tube spacing can be controlled by the preparation conditions, such as the anodization potential, time, and temperature, and the electrolyte composition (water content, cation size, conductivity, and viscosity) (Hagfeldt et al., 2010). In 2005, the first report on dye-sensitized TiO<sub>2</sub> nanotubes appeared (Macak et al., 2005) and the tubes were grown by Ti anodization in two different forms as “long” tubes (tube lengths ~2.5 μm) and “short” tubes (tube lengths ~500 nm), as shown in Fig. 6. Clearly sub-bandgap sensitization with Ru-dye (N3) was successful and led to considerable incident photon-to-current conversion efficiency (IPCE: up to 3.3%). They suggested that main factors that affect IPCE in the visible range were the structure of the tube (anatase better than amorphous), the dye concentration and the tube length. The increase in dye concentration and/or tube length leads to an increase in IPCE, which can be ascribed to a higher packing density of the dye on TiO<sub>2</sub> surface with a higher concentration and a higher light absorption length. So it turns out that for the longer tubes, a significantly lower dye concentration is needed to achieve maximum IPCE values.

TiO<sub>2</sub> nanotubes can also be obtained by anodization of aluminum films on TCO and subsequent immersion in a titanium precursor solution, followed by sintering in a furnace at 400 °C. The alumina template is then removed by immersing the samples in 6 M NaOH solution. Kang (Kang et al., 2009) fabricated highly ordered TiO<sub>2</sub> nanotubes using such nanoporous alumina template method. Such nanotubes with 15 μm lengths were heat treated at 500 °C for 30 min and soaked in N3 dye for 24 h. DSC based on the nanotubes showed a conversion efficiency of as high as 3.5% and a maximum IPCE of 20% at 520 nm.

In order to improve the overall solar cell efficiency, the amount of dye adsorbed by a unit solar cell volume needs to be higher enough. TiCl<sub>4</sub> treatment is an effective way to achieve a higher surface area for nanotube-based photoanodes. Roy et al. (Roy et al., 2009) investigated the effect of TiCl<sub>4</sub> treatments on the conversion efficiency of TiO<sub>2</sub> nanotube arrays. Typical morphology characterizations obtained for nanotube layers before and after this treatment are shown in Fig. 7. The results clearly show that by an appropriate

treatment, the inner as well as the outer wall of TiO<sub>2</sub> nanotubes are covered with a ~25 nm thick nanoparticle coating of TiO<sub>2</sub> nanoparticles with diameter of about 3 nm. This leads to a significant increase in surface area and therefore more dye can be adsorbed to the nanotube walls. Thus, the power conversion efficiency improves from 1.9% for untreated nanotubes to 3.8% for treated nanotubes.

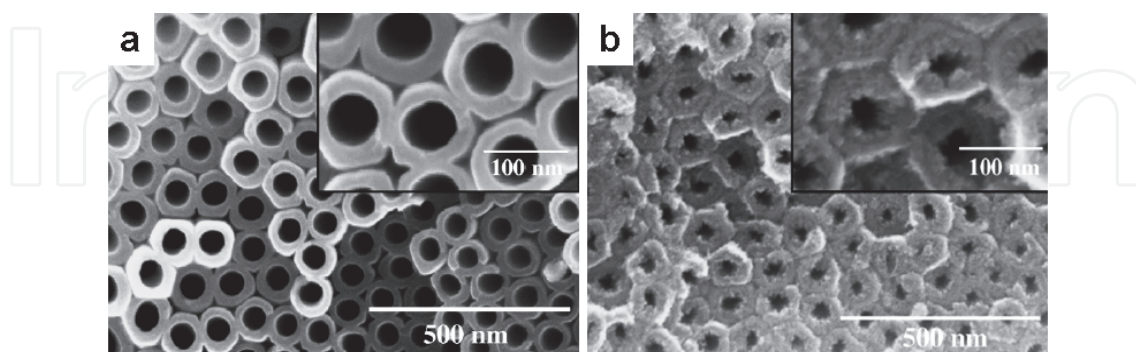


Fig. 7. Influence of TiCl<sub>4</sub> treatment: SEM images of TiO<sub>2</sub> nanotubes (a) before and (b) after TiCl<sub>4</sub> treatment (Roy et al., 2009).

### 2.3.2 ZnO nanotubes

ZnO nanotube arrays have been prepared by different methods for DSCs. There are chiefly three kinds of methods. Firstly, atomic layer deposition is an interesting technique to prepare well-defined and ordered ZnO nanotubes. For example, Martinson et al. (Martinson et al., 2007) reported ZnO nanotube photoanodes through atomic layer deposition in the pores of anodic aluminum oxide (AAO) membrane. However, the surface area of ZnO nanotubes is also very low due to a limit of the available size and pore density of the AAO membranes. Secondly, chemical etching is also effective for fabricating ZnO nanotubes, which involves two steps of process: a first growth of ZnO nanorods and a consequent treatment in alkaline solution; the latter is to convert the nanorods into nanotube structure through a chemical etching. Han et al (Han et al., 2010) fabricated high-density vertically aligned ZnO nanotube arrays on TCO substrates by such simple and facile chemical etching process from electrodeposited ZnO nanorods. The nanotube formation was rationalized in terms of selective dissolution of the (001) polar face. And the morphology of the nanotubes can be readily controlled by electrodeposition parameters for the nanorod precursor. DSC based on 5.1  $\mu\text{m}$ -length ZnO nanotubes exhibited a power conversion efficiency of 1.18%. The conversion efficiency is generally low, which probably results from a fact that the length of ZnO nanotubes is limited by the fabrication method based on an etching mechanism. During the etching treatment, an accompanying dissolution of the ZnO occurs simultaneously and thus leads to a shortening of the nanorods (Zhang & Cao, 2011). At last, electrochemical deposition can also be used to directly prepare ZnO nanotube on TCO glass. Prof. Tang group reported for the first time the electrochemical deposition of large-scale single-crystalline ZnO nanotube arrays on TCO glass substrate from an aqueous solution (Fig. 8a) (Tang et al., 2007). The nanotubes had a preferential orientation along the [0001] direction and hexagon-shaped cross sections. The growth mechanism of ZnO nanotubes was investigated (Fig. 8b). They believed that the key growth step is the formation of oriented nanowires and their self-assembly to hexagonal circle shapes. The nanowires initiated subsequent growth of nanotubular structure. But not all the nanowire circle planes are

parallel to the horizontal plane because of the roughness of F-SnO<sub>2</sub> surface. Some nanotubes have certain angles with the substrate. This nanotube array has great potential for the application in DSCs.

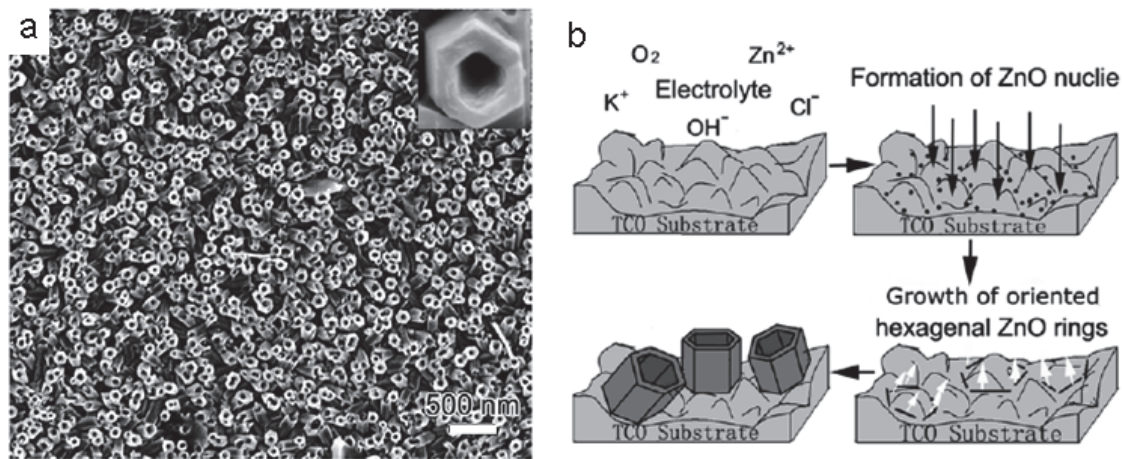


Fig. 8. Surface morphology of ZnO nanotube film (a) and illustration of the growth mechanism of ZnO nanotube array (b). (Tang et al., 2007)

### 3. The application of inorganic nanomaterials in photocathodes

The photocathode, namely counter electrode (CE) where the regeneration of the charge mediator (typical reaction:  $I_3^- + 2e^- (\text{catalyst}) \rightarrow 3I^-$ ) takes place, is one of the most important components in DSCs. The task of CE is twofold: firstly, it transfers electrons arriving from the external circuit back to the redox system (Fig. 9a), and secondly, it catalyzes the reduction of the redox species (Fig. 9b). In order to obtain an effective CE, main requirements for a material to be used as CE are good catalytic activity for the reaction ( $I_3^-/I^-$ ), a low charge transfer resistance, chemical/electrochemical stability in the electrolyte system used in the cell, mechanical stability and robustness.

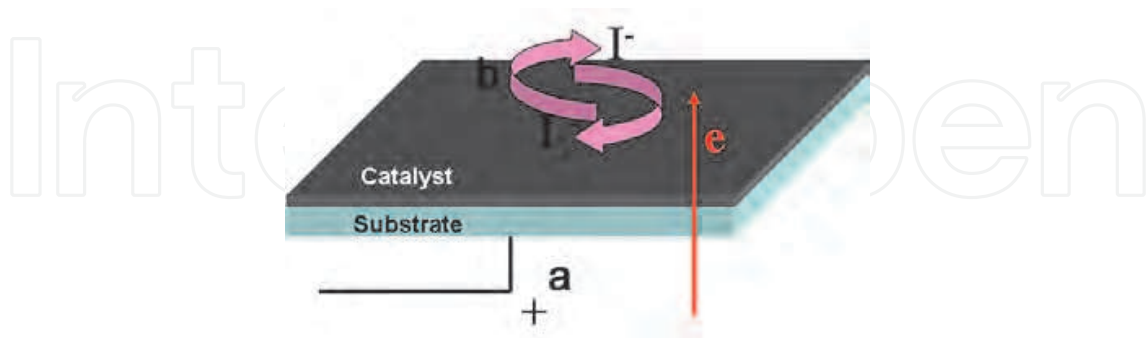


Fig. 9. Schematic representation of the counter electrode based on a  $I^-/I_3^-$  redox couple.

At present, many kinds of CEs have been introduced, for example, metal material CEs, carbon material CEs, conducting polymer CEs, hybrid material CEs, and metallic compound nanomaterial CEs. Since each kind of CEs has their own unique advantages and disadvantages, the CE is chosen according to the particular application of DSCs. For example, the noble metal Pt CE is extremely expensive for large-scale production and may

be corroded by the iodide solution, but for 'champion cells' one must choose this highly catalytic CE with the lowest possible sheet resistance and a high rate of reduction of the redox electrolyte to speed up the reaction ( $I_3^- + 2e^- \rightarrow 3I^-$ ). For power-producing windows or metal-foil-supported DSCs, one must employ a transparent counter electrode, e.g. a small amount of platinum deposited on TCO glass. On the other hand, large solar conversion systems producing electric power on the terawatt scale will prefer materials that are abundantly available. Carbonaceous material CE will be a good choice due to their advantages including good catalytic properties, electronic conductivity, corrosion resistance towards iodine, high reactivity, and abundance. In this section, we briefly introduce three kinds of inorganic nanomaterials as CEs with respect to their application in DSCs, including noble metal materials, carbon materials and metallic compounds nanomaterials.

### 3.1 Metal materials CEs

Up to now, noble metal-loaded substrates have already been widely used as the standard for the CE of DSCs, due to their unique properties, including (1) high electrochemical activity that can reduce the voltage loss due to charge-transfer overpotential of CE; (2) a low charge transfer resistance which can lead to minimum energy loss. A thin layer of noble metals, e.g. Pt, Au, is well established as the catalyst on CE substrate, such as TCO glass and metal foil. One of the important roles of noble metal in CE is to catalyze the reduction of triiodide ( $I_3^-$ ) ions. This means that the available catalytic surface in the electrode plays a crucial role in determining the overall device current. So the rough/porous electrodes, which are characterized by a higher surface, are expected to assure a higher number density of catalytic sites. It is obvious that the use of metal nanoparticle film results in CE with high surface area. Therefore, the preparation methods of noble metal films will influence the final film structure/properties.

Generally all the synthetic methods of the noble metal film are roughly divided into two categories: the physical and chemical approaches. The difference between the two approaches arises from the starting point in the synthetic route to prepare the films. For the physical approaches, the film is prepared by the macroscopic precursors through subsequent subdivision in ever smaller particles by strong milling of solids or through lithographic processes including sputtering, laser ablation, vapor phase deposition, lithography, etc. While the chemical approaches start from their atomic and molecular precursors, through chemical reactions and modulating their self-assembling in order. The physical approaches (Terauchi et al., 1995) are generally quite expensive and resource-consuming, while chemical methods are generally cheaper and better fit for large scale applications. Moreover, since chemical methods allow in principle the control at a molecular level, they allow a fine size and polydispersity control and can be implemented to prepare 2D and/or 3D nanoparticle arrays to enhance the available catalytic site.

The catalytic activity is expressed in terms of the exchange current density ( $J_0$ ), which is calculated from the charge-transfer resistance ( $R_{ct}$ ) using the equation  $R_{ct} = RT/nFJ_0$ , in which  $R$ ,  $T$ ,  $n$ , and  $F$  are the gas constant, temperature, number of electrons transferred in the elementary electrode reaction ( $n = 2$ ) and Faraday constant, respectively. Yoon et al (Yoon et al., 2008) used Nyquist plots to investigate  $R_{ct}$  on platinized TCO CEs prepared by either the electrochemical deposition (ED) method, the sputter-deposited (SD) method, or the thermal deposited (TD) method. The Nyquist plots suggest qualitatively that  $R_{ct}$  of a cell increases in the order of  $R_{ct}$  of ED-Pt film  $<$   $R_{ct}$  of SD-Pt film  $<$   $R_{ct}$  of TD-Pt film. The DSC fabricated with the ED-Pt CE rendered the highest power conversion efficiency of 7.6%, compared with

approximately 6.4% of the cells fabricated with the SD-Pt or most commonly-employed TD-Pt CEs. The improved performance of DSC with the ED-Pt CE is attributed to the improved catalytic activity of the reduction reaction ( $I_3^- + 2e^- \rightarrow 3I^-$ ) and the decreased charge transfer resistance at CE/electrolyte interface. Hauch et al (Hauch & Georg, 2001) also used impedance spectra to investigate  $R_{ct}$  on platinized TCO CEs prepared by either the electron-beam evaporation (EB), SD or TD method. The 450 nm thick platinum electrode prepared by SD method gave the lowest  $R_{ct}$  of 0.05 ohm/cm<sup>2</sup>. The TD of a Pt film (<10 nm thick), using H<sub>2</sub>PtCl<sub>6</sub> as a precursor on a TCO substrate, produced a low  $R_{ct}$  of 1.3 ohm/cm<sup>2</sup> comparable to the  $R_{ct}$  of the 40 nm thick sputtered Pt, confirming the superiority of the TD method.

### 3.2 Carbon material CEs

DSC is well known as potentially low-cost photovoltaic devices (Gratzel, 2004); from this perspective, the application of low-cost materials should be important. Low-cost carbon is the second most widely studied material for CEs after metal materials. Carbonaceous materials feature good catalytic properties, electronic conductivity, corrosion resistance towards iodine, high reactivity and abundance (Wroblowa & Saunders, 1973). Since the fact that Kay and Grätzel found good electrocatalytic activity of graphite/carbon black mixture in 1996 (Kay & Gratzel, 1996), various kinds of carbon are studied, such as hard carbon spherules (Huang et al., 2007), activated carbon (Imoto et al., 2003), mesoporous carbon (Wang et al., 2009a), nanocarbon (Ramasamy et al., 2007), single-walled carbon nanotubes (Suzuki et al., 2003), multiwalled carbon nanotubes (MWNTs) (Seo et al., 2010), carbon fiber (Joshi et al., 2010) and graphene nanoplates (Kavan et al., 2011). Nevertheless carbonaceous electrodes which would be superior to Pt were reported only rarely for certain kinds of activated carbon (Imoto et al., 2003). This result is mainly attributed to the poor catalytic activity for I<sub>3</sub><sup>-</sup>/I<sup>-</sup> redox reaction. In addressing this issue, several optimizing methods have been developed, such as increasing the surface area, functionalizing the carbon materials to get more active sites for I<sub>3</sub><sup>-</sup>/I<sup>-</sup> redox reaction.

To achieve a comparable activity to platinum, carbon-based CEs must have sufficiently high surface area. Although carbonaceous electrodes have poor catalytic activity for I<sub>3</sub><sup>-</sup>/I<sup>-</sup> redox reaction, its exceptional surface area and conductivity, such as mesoporous carbon and graphene, have been shown to be quite effective and in some cases even exceeded the performance of platinum. Imoto et al (Imoto et al., 2003) compared several types of activated carbon with different surface areas ranging from 1000 m<sup>2</sup> g<sup>-1</sup> to 2000 m<sup>2</sup> g<sup>-1</sup> as the CE catalyst, assessing in addition the activity of several different types of activated carbon, glassy carbon, and graphite. The surface area of the glassy carbon and graphite was three orders of magnitude lower than those of the activated carbon catalysts. In the preparation of the latter electrodes, a certain amount of carbon black was included. In their results, the electrodes consisting of the lower sheet resistance materials, graphite and glassy carbon, gave lower  $J_{sc}$  values and fill factors, indicating the importance of the roughness of the carbon materials in achieving a better performance. They demonstrated an improvement in the  $J_{sc}$  and FF with increasing thickness (>30 μm) of the carbon material. Robert et al (Sayer et al., 2010) used the dense, vertical, undoped MWCNT arrays grown directly on the electrode substrate as CEs and got a greater short-circuit current density and higher efficiency than DSCs with Pt CE. The improved performance is attributed to increased surface area at the electrolyte/counter electrode interface that provides more pathways for charge transport. Prakash et al (Joshi et al., 2010) investigated the electrospun carbon nanofibers as CEs. The results of electrochemical impedance spectroscopy (EIS) and cyclic voltammetry measurements

indicated that the carbon nanofiber based CEs exhibited low charge-transfer resistance, large capacitance, and fast reaction rates for triiodide reduction. Joseph et al (Roy-Mayhew et al., 2010) found that functionalized graphene sheets with oxygen-containing sites perform comparably to platinum. Using cyclic voltammetry, they demonstrated that tuning the graphene sheets by increasing the amount of oxygen-containing functional groups can improve its apparent catalytic activity.

### 3.3 Metal compounds CEs

A possible approach is to utilize transition-metal compounds with similar properties to those of noble metals (Shi et al., 2004). Compared with metallic materials, transition-metal compounds have a great potential to be used as cost-effective CEs in DSCs due to their unique properties including a broad variety of low cost materials, a good plasticity, a simple fabrication, high catalytic activity, selectivity, and good thermal stability under rigorous conditions (Wu et al., 2011a). Recently, several kinds of transition-metal compounds CEs, e.g., nitrided Ni particle film, TiN nanotube arrays, MoC have been reported in DSCs which have a conversion efficiency superior to Pt.

Jiang et al (Jiang et al., 2009) used TiN nanotube arrays as CE in DSC for the first time, and the resulting DSC had photovoltaic performances comparable to those using the conventional TCO/Pt counter electrodes, which should be attributed to the obviously lower charge-transfer resistances at the CE/electrolyte interfaces and ohmic internal resistances. The exciting photovoltaic performances comparable to Pt CE inspire the researches on the transition-metal compounds used as the new kind of CEs. They also investigated the surface-nitrided nickel film as a low cost CE material, and the resulting DSCs presented an excellent photovoltaic performance competing with that with the conventional Pt CE (Jiang et al., 2010). Molybdenum and tungsten carbides embedded in ordered mesoporous carbon materials (MoC-OMC, WC-OMC) as well as Mo<sub>2</sub>C and WC were prepared respectively by Wu et al (Wu et al., 2011a). They demonstrated that DSCs equipped with optimized MoC-OMC, WC-OMC, Mo<sub>2</sub>C, and WC showed higher power conversion efficiency than those devices with a Pt CE. Very recently, they have developed another kind of CE, tungsten oxides, based on their excellent catalytic activity (Wu et al., 2011b). They found that WO<sub>2</sub> nanorods showed excellent catalytic activity for triiodide reduction, and the DSC based on a WO<sub>2</sub> CE reached a high energy conversion efficiency of 7.25%, close to that of the DSC using Pt CE (7.57%). Their results exhibit that tungsten oxides are promising alternative catalysts to replace the expensive Pt in DSCs system. Wang et al (Wang et al., 2009b) have demonstrated, for the first time, that CoS is very effective in catalyzing the reduction of triiodide to iodide in a DSC, superseding the performance of Pt as an electrocatalyst. They deposited the CoS layer on a flexible ITO/polyethylene naphthalate films. CoS based flexible and transparent CEs not only matched the performance of Pt as a triiodide reduction catalyst in DSCs, but also showed excellent stability in ionic liquids-based DSCs under prolonged light soaking at 60 °C. Clearly, the CoS has an advantage for large scale application as being a much more abundant, transparent and cheaper CE.

## 4. The application of inorganic nanomaterials in quasi-solid/solid-state electrolytes

The power conversion efficiency of DSCs with organic solvent-based electrolyte was reported to exceed 11% (Gratzel, 2004). However, the presence of organic liquid electrolytes

in cells causes problems, such as leakage, evaporation of solvent, high-temperature instability, and flammability, and therefore results in practical limitations to sealing and long-term operation. At present, many attempts have been made to substitute liquid electrolytes with solid state electrolytes (e.g. p-type semiconductors, organic hole-transport materials, solid polymer electrolytes, and plastic crystal electrolytes) or quasi-solid-state electrolytes (e.g. polymer gel, low-molecular-weight gel). Here, we focus our attention on the application of inorganic nanomaterials in quasi-solid/solid-state electrolytes, including p-type semiconductor nanoparticles as solid-state electrolytes and solidification of liquid electrolyte by inorganic nanoparticles.

#### 4.1 p-type semiconductor nanoparticles as solid-state electrolytes

P-type semiconductors are the most common hole-transporting materials to fabricate solid-state DSCs. Several aspects are essential for any p-type semiconductor in a DSC: (a) It must be able to transfer holes from the oxidized dye; (b) It must be able to be deposited within the porous TiO<sub>2</sub> nanocrystal layer; (c) A method must be available for depositing the p-type semiconductors without dissolving or degrading the dye on TiO<sub>2</sub> nanocrystal; (d) It must be transparent in the visible spectrum, otherwise, it must be as efficient in electron injection as the dye. Copper-based materials, especially CuI and CuSCN (Tennakone et al., 1995), are found to meet all these requirements. CuI and CuSCN share good conductivity in excess of 10<sup>-2</sup> Scm<sup>-1</sup>, which facilitates their hole conducting ability (Smestad et al., 2003), hence, they have been widely used as complete hole-transporting layer for fabricating solid-state DSCs. Tennakone et al (Tennakone et al., 1995) first reported a nano-porous solid-state DSC based on CuI in 1995. DSCs were fabricated by sandwiching a monolayer of the pigment cyanidin adsorbed on nano-porous n-TiO<sub>2</sub> film within a transparent polycrystalline film of p-CuI, filling the intercrystallite pores of the porous n-TiO<sub>2</sub> film. The short-circuit current density reached about 1.5–2.0 mAcm<sup>-2</sup> in sunlight (about 800 Wm<sup>-2</sup>), however, they found that the polarization arising from mobile Cu<sup>+</sup> ions tends to decrease the open-circuit voltage of the cell. By replacing cyanidin with a Ru-bipyridyl complex dye, they (Tennakone et al., 1998) then fabricated a solid-state DSC with the structure of TiO<sub>2</sub>/Ru(II)(dcbpy)<sub>2</sub>(SCN)<sub>2</sub>/CuI in 1998. The efficiency and the stability of the solid-state DSC was less than those of the typical DSCs. They attributed it to the loosening of the contact between the p-type semiconductor and the dye monolayer, and to short-circuiting across the voids in the nanoporous TiO<sub>2</sub> film, which allows direct contact between CuI and the tin oxide surface. To solve this issue, they (Kumara et al., 2002) incorporated a small quantity (~10<sup>-3</sup> M) of 1-methyl-3-ethylimidazolium thiocyanate (MEISCN) into the coating solution (i.e., CuI in acetonitrile) and the stability of the CuI-based DSC was greatly improved. In this case, MEISCN acted as a CuI crystal growth inhibitor, which enables filling of the pores of the porous matrix, resulting in the formation of more complete and secure contacts between the hole collector and the dyed surface. Meng et al (Meng et al., 2003) also utilized MEISCN to control the CuI crystal growth and act as a protective coating for CuI nanocrystals, improving the cells' efficiency to 3.8% with improved stability under continuous illumination for about 2 weeks. Another alternative for solid-state DSCs is CuSCN. O'Regan et al (O'Regan & Schwartz, 1995) used CuSCN as a hole transport layer, and demonstrated that CuSCN is a promising candidate material as the hole-conducting layer. They found the UV illumination created an interfacial layer of (SCN)<sub>3</sub><sup>-</sup>, and/or its polymerization product (SCN)<sub>x</sub>, between the TiO<sub>2</sub> and the CuSCN, causing a dramatic improvement in the efficiency of DSCs (O'Regan & Schwartz, 1998). Later, they (O'Regan et al., 2000) substituted TiO<sub>2</sub> for ZnO, fabricating

ZnO/dye/CuSCN solar cell with a conversion efficiency of 1.5%. In 2005, they (O'Regan et al., 2005) made another solid-state DSC with the structure of TiO<sub>2</sub>/dye/CuSCN with thin Al<sub>2</sub>O<sub>3</sub> barriers between the TiO<sub>2</sub> and the dye. It is noteworthy that the Al<sub>2</sub>O<sub>3</sub>-treated cells showed improved voltages and fill factors but lower short-circuit currents. Nevertheless, the performance of DSCs with CuSCN is still lower than that of cells utilizing CuI, probably due to the relatively lower hole conductance.

In summary, compared to a liquid electrolyte DSC, the solid-state counterpart presents a relatively low conversion efficiency, which is probably due to three reasons (Kron et al., 2003): (a) the less favorable equilibrium Fermi-level position in the TiO<sub>2</sub>; (b) poor conductivity of hole-transporting materials; (c) the much larger recombination probability of photogenerated electrons from the TiO<sub>2</sub> with holes as compared to recombination with the I<sup>-</sup>/I<sub>3</sub><sup>-</sup> redox couple. So it is necessary to make further efforts to design new and more efficient inorganic nanomaterial electrolytes for DSCs.

#### 4.2 Solidification of liquid electrolyte by inorganic nanoparticles

Room-temperature ionic liquids (RTILs) such as imidazolium iodide have been widely used in DSCs as a solvent and a source of I<sup>-</sup> or other ions, because of their favorable properties such as thermal stability, nonflammability, high ionic conductivity, negligible vapor pressure, and a possible wide electrochemical window. However, the fluidity of RTIL-based electrolytes, resulting in difficulty in seal, is still an obstacle for long-term operation. To reduce its fluidity, combination of RTILs with a framework material including small-molecular organogels, inorganic nanoparticles, and polymer, has been attempted by many groups.

Among these framework materials, inorganic nanoparticles have drawn more attention. In 2003, silica nanoparticles were used for the first time to solidify ionic liquids by Prof. Grätzel group (Wang et al., 2003a). The presence of silica nanoparticles has no adverse effect on the conversion efficiency, and the ionic liquid-based quasi-solid-state electrolytes are successfully employed for fabricating DSC with a conversion efficiency of 7%. This means that quasi-solid-state electrolytes offer specific benefits over the ionic liquids and will enable the fabrication of flexible, compact, laminated quasi-solid-state devices free of leakage and available in varied geometries. In addition, for their pore structures (2-50 nm) and large surface area, mesoporous materials may solidify liquid electrolytes and provide favourable channels for the triiodide/iodide diffusion. By using the mesoporous SiO<sub>2</sub> material (SBA-15) as the framework material, Yang et al (Yang et al., 2005) fabricated a quasi-solid-state electrolyte and then fabricated DSC with a energy conversion efficiency of 4.34%. ZnO nanoparticle also can be used to solidify the liquid electrolyte. For example, Huang group (Xia et al., 2007) used ZnO nanoparticles as a framework to form a quasi-solid-state electrolyte for DSC. The quasi-solid-state DSC with the quasi-solid-state electrolyte showed higher stability in comparison with that of the liquid device, and gave a comparable overall efficiency of 6.8% under AM 1.5 illumination.

Thermal stability is an urgent concern for quasi-solid DSCs based on RTIL gel electrolytes. Some room-temperature quasi-solid-state electrolytes usually become liquid at high temperature (40–80 °C), for example, 3-methoxypropionitrile (MPN)-based polymer gel electrolyte (viscosity: 4.34 MPa s at 80 °C) (Wang et al., 2003b) and plastic crystal electrolytes (m.p. 40–45 °C) (Wang et al., 2004). Since the working temperature of DSCs may reach 60 °C under full sunlight, it is necessary that at high temperature (60–80 °C), the electrolytes are still in the quasi-solid or solid state and that the DSCs maintain high overall energy-



conversion efficiency (>4%). We (Chen et al., 2007b) have developed a succinonitrile-based gel electrolyte by introducing a hydrogen bond (O-H...F) network upon addition of silica nanoparticles and BMI·BF<sub>4</sub> (1-Butyl-3-methylimidazolium tetrafluoroborate) to succinonitrile. When the content of fumed silica nanoparticles was over 5 wt%, the succinonitrile-BMI·BF<sub>4</sub>-silica system became a gel, and the succinonitrile-BMI·BF<sub>4</sub>-silica (7 wt%) system still remained in the gel state even at 80 °C, as shown in the inset of Fig. 10, which confirms that the addition of silica nanoparticles and BMI·BF<sub>4</sub> is critical for the gelation and thermostability of succinonitrile-based electrolytes. The appropriate addition of BMI·BF<sub>4</sub> and silica nanoparticles in this gel electrolyte can greatly improve the thermostability but has no adverse effects on the conductivity, ionic diffusion coefficients and the cell performance. Moreover, the relatively high succinonitrile content in the electrolyte is also very important because the electrolyte without succinonitrile has very low conductivity and results in poor cell performance. Herein, the obtained succinonitrile-based gel electrolyte satisfies the need for both thermostability and high conductivity in electrolytes. DSCs with this gel electrolyte showed power conversion efficiencies of 5.0–5.3% over a wide temperature range (20–80 °C). Furthermore, the aging test revealed that the cell still maintained 93% of its initial value for the conversion efficiency after being stored at 60 °C for 1000 h, indicating an excellent long-time durability.

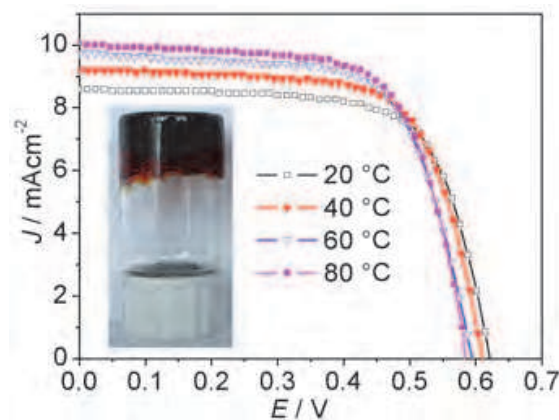


Fig. 10. Photos of succinonitrile-BMI·BF<sub>4</sub>-silica (silica: 7 wt% of succinonitrile-BMI·BF<sub>4</sub>) at 80 °C (Chen et al., 2007b).

## 5. Inorganic nanomaterials as light-absorbing materials

### 5.1 Semiconductor QDs

The emergence of semiconductor quantum dots (QDs) has opened up new ways to utilize them as a possible replacement for ruthenium complex dyes (sensitizers) in DSCs. QDs have many advantages including good thermal stability under rigorous conditions, tunable bandgaps, sharp absorption onset, large absorption coefficients and low cost etc. Hence, the QD-sensitized solar cells (QD-SCs) have attracted more attention. In the past few years, a rapid increase of the conversion efficiency of QD-SCs has been reported, reaching values of around 4–5% at 1 sun (Chang et al., 2010). The efficiency of QD-SC still lags behind those of DSC; however, a further performance improvement for QD-SCs can be anticipated.

Recently, various QDs (CdSe (Levy-Clement et al., 2005), PbSe (Leschkies et al., 2009), CuInS<sub>2</sub> (Kaiser et al., 2001), etc.) as the sensitizer have been proposed, and various strategies have been developed for maximizing photoinduced charge separation and electron transfer

processes to improve the power conversion efficiency. This section aims to introduce the recent developments in the synthesis methods of high quality QDs and the performance optimization strategies of QD-SC.

### 5.1.1 Synthesis of QDs

QDs used as sensitizer in DSC have been fabricated by using two fundamentally different approaches. The first and most common route employs the *in situ* preparation of QDs onto the nanostructured semiconductor metal oxide film. The second approach is *ex situ* growth approach, which can take advantage of the tremendous developments in controlling the growth of monodisperse, highly crystalline and diverse QDs. This method is to synthesis the QDs independently, and subsequently to attach the pre-synthesized QDs to the photoanode by a bifunctional linker molecule or direct adsorption. Both of these preparation methods have their limitation respectively, hence it is still necessary to develop a new method in the future.

#### 5.1.1.1 *In situ* preparation of QDs

The *in situ* preparation method, where the QDs are directly generated on the surface of metal oxide film electrode, mainly includes chemical bath deposition (CBD) (Diguna et al., 2007) and successive ionic layer adsorption and reaction (SILAR) (Lee et al., 2009a). There are many of advantages of the *in situ* deposition approaches. Firstly, the *in situ* deposition approaches are easy to process since it does not need any expensive equipment and multiple complicated steps. Secondly, the QDs are in direct electronic contact with metal oxide, which not only makes the QDs good anchoring to the electrodes but also shortens the electron diffusion length. Thirdly, they can easily produce metal oxide films with high surface coverage of the sensitizing QDs, which increases the absorption of light. However, this method still has several intrinsic limitations. For example, it is difficult to control chemical composition, crystallinity, size distribution and surface properties of QDs, which may hamper the effective exploitation of QDs advantages. .

For CBD method, QDs are deposited *in situ* by immersing the wide-bandgap nanostructured electrode (usually metal oxide) into a solution that contains the cationic and anionic precursors, which react slowly in one bath under different temperature. Most of the sulfides and selenides can be prepared by this method. Lee et al developed a method coupling self-assembled monolayer and CBD, as well as a modified CBD process performed in an alcohol system to assemble CdS into a TiO<sub>2</sub> film (Lin et al., 2007). These modified processes have been proved to be efficient for CdS QD-SC, and CdS QD-SCs exhibit a power conversion efficiencies of 1.84% and 1.15% respectively for iodide/triiodide and polysulfide electrolytes (Lin et al., 2007).

In the SILAR approach, the cationic and anionic precursor solution is placed in two vessels respectively. Firstly, the nanostructured electrode is immersed into the solution containing the metal cation, and then the nanostructured electrode absorbing the metal cation on the surface is taken out from the metal cation solution and dip into the second precursor solution containing the anion. After the second rinsing step, the deposition cycle completes. The average QD size can be controlled by the number of deposition cycles. This method has been used in particular to prepare metal sulfides, but recently it has been expanded to metal selenides and tellurides. For example, Grätzel et al deposited the CdSe and CdTe QDs *in situ* onto mesoporous TiO<sub>2</sub> films using SILAR approach (Lee et al., 2009b). After some

optimization of these QD-sensitized TiO<sub>2</sub> films in solar cells, over 4% overall efficiency was achieved at 100 W/m<sup>2</sup> with about 50% IPCE at its maximum (Lee et al., 2009b).

### 5.1.1.2 *Ex situ* growth approach

The *ex situ* growth approach is based on a two-step process, whereby QDs are first independently synthesized using established colloidal synthesis method and then QDs are subsequently linked on to the metal oxide film electrodes to achieve effective QD-electrode junctions that would promote charge separation while minimizing surface trapping and hence losses (Kamat, 2008). This approach can take advantage of the tremendous developments in controlling over the chemical, structural, and electronic properties of QDs compared to the *in situ* approaches. However, since QDs, unlike dyes, do not possess an anchoring functional group for coupling to the metal oxide film surface, this approach provides limited control over the metal oxide film sensitization process and degree of QD-metal oxide film electronic coupling. In addition, the as prepared QDs are typically passivated with a layer of organic ligands, such as tri-*n*-octylphosphine oxide (TOPO), aliphatic amines, or acids, which serve as an impediment to effective metal oxide film sensitization and as a barrier to efficient charge transfer across the QD/metal oxide film and QD/electrolyte interfaces.

The first step of the *ex situ* growth approach is the synthesis of the monodisperse QDs (Fig. 11a). The most common synthesis approach is to control the nucleation and growth process of particles in a solution of chemical precursors containing the metal and the anion sources (Overbeek, 1982). In a typical process, the solvent containing molecules (e.g. trioctylphosphine and trioctylphosphine oxide) is heated to 150-350 °C under the vigorously stirred with protective atmosphere, and then the organometallic precursor and related species are injected. Consequently, a large number of nucleation centers are initially formed, and the coordinating ligands in the hot solvent prevent or limit particle growth via Ostwald ripening. Typical reactions used for the synthesis of II-VI (CdSe, CdTe, CdS) (Peng & Peng, 2002), III-V (InP, InAs) (Talapin et al., 2002), and IV-VI (PbSe (Talapin & Murray, 2005)) QDs are outlined by reactions 1-3 (Fig. 11a).

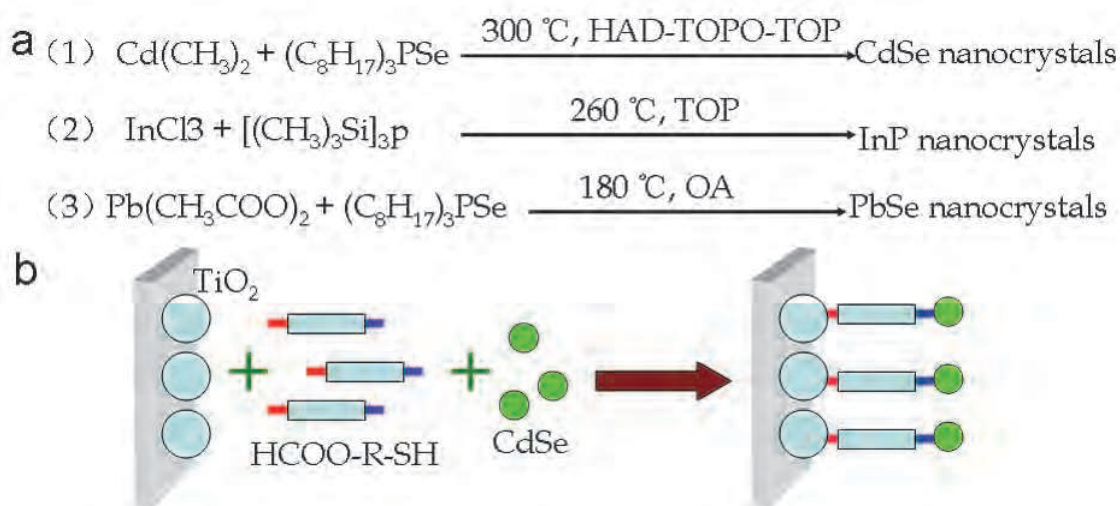


Fig. 11. (a) Typical reactions used for the synthesis of QDs. (b) Scheme of attaching the pre-synthesized QDs to the electrode material by a bifunctional linker molecule (Robel et al., 2006).

The second step of the *ex situ* growth approach is to attach the pre-synthesized QDs to the electrode material by a bifunctional linker molecule (usually HOOC-R-SH, where R is the organic core of the linker) or direct adsorption (Fig. 11b). The carboxyl group attaches to the nanostructured metal oxide film, while the thiol remains free for connecting QDs. Then the modified film is immersed in the QD solution (for several hours or days) for the adsorption of QDs, which typically involves fractional ligand exchange. For instance, Kamat et al (Robel et al., 2006) immersed the TiO<sub>2</sub> films into a solution of acetonitrile containing carboxy alkane thiols (Mercaptopropionic acid, thiolacetic acid and mercaptohexadecanoic acid) for ~4 h as shown in the Fig. 11b. Resulting TiO<sub>2</sub> films functionalized with these bifunctional surface modifiers, were then washed with both acetonitrile and toluene, and transferred to a glass vial containing a suspension of CdSe QDs in toluene. The electrodes were kept immersed in the CdSe solution for approximately 12 h. QDs self-assembly had also been used on dispersed TiO<sub>2</sub> crystals, where the photoelectrode was fabricated after QD sensitization by a pressing route (Ardalan et al., 2011). Direct adsorption was recently proposed for deposition of monodisperse QDs without molecular linkers to the surface of the metal oxide nanostructure. This procedure has already been employed to sensitize TiO<sub>2</sub> with QDs, such as CdSe QDs (Shen et al., 2009), although the obtained photocurrents at 1 sun intensity are low. One possible explanation is that directly adsorbed colloidal QDs provides a low surface coverage of about 14% (Gimenez et al., 2009). It is obvious that higher surface coverage of colloidal QDs on TiO<sub>2</sub> substrate will result in QD-SCs with higher conversion efficiency.

### 5.1.2 Performance optimization of QDs in the QD-SCs

Theoretically, there are many advantages of the QDs for sensitizing the nanoporous oxide film electrode, such as higher absorption of QD coating, greater stability of the semiconductor, and tailoring of optical absorption over a wider wavelength range (Hodes, 2008). Moreover, the demonstration of multiple exciton generation (MEG) by impact ionization in colloidal QDs could push the thermodynamic efficiency limit of these devices up to 44% (Klimov, 2006) instead of the current 31% of the Shockley-Queisser detailed balance limit. Although, up to now, the efficiencies of QD-SCs are far behind those of DSCs (DSC currently exceeds 11% at 1 sun illumination (Cao et al., 2009)), QD-sensitized nanostructured solar cells are attracting increasing attention among researchers and are progressing rapidly to values around 4-5% from quite low conversion efficiencies (Gonzalez-Pedro et al., 2010). Several methods have been developed to optimize the performance of the QD-SCs including (1) tuning of effective bandgaps from visible down to the IR range by changing their sizes and compositions, (2) utilizing the phenomena of MEG, Förster resonance energy transfer (FRET)-based charge collection, and direct charge transfer schemes, and (3) surface treatment.

#### 5.1.2.1 Tuning of bandgaps of QDs

The most striking property of QDs is the massive changes in electronic structure as a function of size. As the size decreases, the electronic excitations shift to higher energy, and the oscillator strength is concentrated into just a few transitions (Murray et al., 1993). Therefore, controlling quantum size confinement in monodisperse QDs is the most obvious method not only to extend the range of the QDs absorbance from the visible to near infrared range but also to align the energy levels with respect to the wide-bandgap nanostructure. Herein, the CdSe QDs and TiO<sub>2</sub> system as a model is introduced for the direction of the optimization. The driving force for the electron separation and transfer is dictated by the

energy difference between the conduction band energies. The conduction band of  $\text{TiO}_2$  is at  $-0.5 \text{ V vs NHE}$ . If we assume the larger CdSe particles have band energy close to the reported value of  $-0.8 \text{ V vs NHE}$ , we can use the increase in bandgap as the increase in driving force for the electron transfer. Since the shift in the conduction band energy is significantly greater than the shift in valence band energy for quantized particles (Norris & Bawendi, 1996), we can expect the conduction band of CdSe QDs to become more negative (on NHE scale) with decreasing particle size. As the particle size decreases from 7.5 to 2.4 nm, the first excitonic peak shifts from 645 nm to 509 nm and the conduction band shifts from  $-0.8 \text{ V vs NHE}$  to  $-1.31 \text{ V}$ , the electron transfer rate improve by nearly 3 orders of magnitude (Robel et al., 2007). PbS nanocrystals have similar properties with the light absorption range extending from visible to near infrared (Hyun et al., 2008).

Another method that can broaden the spectral absorption range is the use of nanocomposite absorbers (Lee & Lo, 2009). Semiconductor QDs are excellent building blocks for more sophisticated nanocomposite absorbers, which the QDs combined with each other with different size or type. The well-known example of the nanocomposite is the combination of CdS and CdSe QDs. The combination can be used as co-sensitizers to provide enhanced performance compared to the use of each individual semiconductor QDs. When CdSe QDs are assembled on a  $\text{TiO}_2/\text{CdS}$  electrode, the co-sensitized electrode ( $\text{TiO}_2/\text{CdS}/\text{CdSe}$ ) has an absorption edge close to that of  $\text{TiO}_2/\text{CdSe}$  electrode but its absorbance is higher than those of  $\text{TiO}_2/\text{CdS}$  and  $\text{TiO}_2/\text{CdSe}$  electrodes both in the short wavelength region ( $<550 \text{ nm}$ ) where both CdS and CdSe are photoactive and long wavelength region (ca. 550–700 nm) which belong to the CdSe due to the complementary effect of the composite sensitizers. When CdS is located between CdSe and  $\text{TiO}_2$ , both the conduction and valence bands edges of the three materials increase in the order:  $\text{TiO}_2 < \text{CdS} < \text{CdSe}$ , which is advantageous to the electron injection and hole recovery of CdS and CdSe. This clearly shows that nanocomposite absorbers can improve these systems through two different beneficial effects. On the one hand, the spectral absorption range can be broadened. On the other, the re-organization of energy levels between CdS and CdSe forms a stepwise structure of band-edge levels (Lee & Lo, 2009).

### 5.1.2.2 Utilizing the phenomena of MEG and energy/charge transfer

MEG can occur when absorption of a high-energy photon leads to production of an excited electron or a hole with an excess energy at least equal to or greater than the QD bandgap ( $E_g$ ). These hot carriers can transfer the entire excess energy, or part of it, to one or more valence electrons, and excite them across the bandgap. In this way, absorption of a single photon leads to generation of two or more electron-hole pairs. The quantum yield for exciton generation is defined as the average number of electron-hole pairs produced by absorption of a single photon. The analogous phenomenon of multiple charge carrier generation per photon in bulk semiconductors is termed impact ionization and is considered an inverse of Auger recombination. MEG in QDs has mostly been described as a coherent process in which single and multi-exciton states are coupled via the Coulomb interaction (Beard et al., 2007). In 1982 it was recognized that it could be possible to increase solar cell efficiency for a single junction by utilizing MEG (Ross & Nozik, 1982). Under 1 sun AM1.5 spectrum the theoretical efficiency of a MEG-enhanced cell is over 44% (Klimov, 2006). Among the various QDs materials, PbS and PbSe are good candidates for solar cells, because they not only can be made to overlap the solar spectrum optimally, which the absorption wavelength of the first exciton peak can easily be extended into the infrared by controlling

their sizes (Vogel et al., 1994), but also show that two or more excitons can be generated with a single photon of energy greater than the bandgap (Ellingson et al., 2005). PbSe and PbS QDs have been shown to have quantum yields above 300% (Ellingson et al., 2005) and even above 700% (Schaller et al., 2006).

As a new approach, long range FRET, also known as electronic energy transfer, has been also utilized in the DSCs recently. The donor dye molecules, which are added to the redox solution, upon absorption of light, transfer the excitation energy to an acceptor dye adsorbed on the electrode followed by the standard charge separation process. However, the donor molecules are heavily quenched in the liquid electrolytes (Shankar et al., 2009). Similar geometries using other sensitizers, such as inorganic semiconductor nanocrystals, have been proposed (Chen et al., 2008). QDs have the advantage of a broad absorption spectrum, stretching from the band edge to higher energies, in contrast with the narrow absorption spectra typically exhibited by molecular dyes (Buhbut et al., 2010). The use of FRET has been contemplated as an alternative mechanism for charge separation and a way to improve exciton harvesting by placing the exciton close to the heterojunction interface (Liu et al., 2006). In inorganic QD-DSCs, the use of FRET to transfer the exciton generated in the QD to a high mobility conducting channel, such as a nanowire or a quantum well, has been proposed as a way to bypass the traditional limitations of charge separation and transport (Lu & Madhukar, 2007). Very recently, Sophia et al (Buhbut et al., 2010) presented a design which combines the benefits of QDs in terms of their broad absorption spectrum with the evolved charge transfer mechanism of DSC. They demonstrated that QDs serving as “antennas” could enhance light absorption, broaden the absorption spectrum, increase the number of photons harvested by solar cell effectively and funnel absorbed energy to nearby dye molecules via FRET successfully. Their design introduced new degrees of freedom in the utilization of QDs sensitizers for solar cells. In particular, it opens the way toward the utilization of new materials whose band offsets do not allow direct charge injection.

### 5.1.2.3 Surface treatment

Regarding the surface treatment, it is important to remark a significant difference between molecular dyes and semiconductors used as sensitizers. As suggested by Hodes (Hodes, 2008), the probable existence of surface states in the sensitizing semiconductor is a major difference between DSCs and QD-SCs. These surface states have been widely studied in colloidal QDs and can be detected by different techniques such as photoluminescence or scanning tunnelling microscopy. The observed behaviors strongly depended on the surface treatment or the type of capping ligand (Frederick & Weiss, 2010). Surface modification by dipoles provides a simple and efficient way to shift the QD energy level. For monodisperse QDs, fractional exchange of the capping ligands by molecular dipoles can be used to shift the electronic QD states with respect to their environment in a systematic fashion, as shown in the Fig. 12 (Ruhle et al., 2010).

## 5.2 Rare-earth up-converting nanophosphors

Light-absorbing materials developed for solar cells, such as silicon and dyes, can not efficiently absorb near infrared light. In contrast, some rare-earth phosphors, especially those co-doped with  $\text{Yb}^{3+}$  and  $\text{Er}^{3+}$ , can efficiently absorb near infrared light, such as 980-nm laser light, after which they exhibit up-converted luminescence in the visible range (Heer et al., 2004). Doping of rare-earth materials into solar cells has been demonstrated as a better

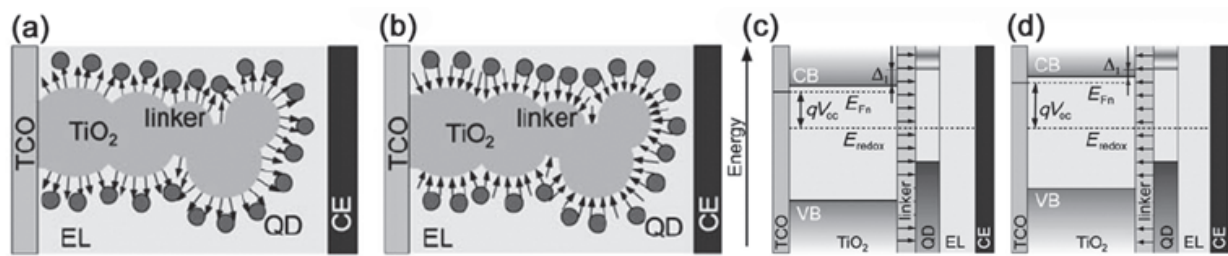


Fig. 12. (a) Schematic drawing of a mesoporous TiO<sub>2</sub> film, covered with linker molecules with a molecular dipole pointing towards the QD monolayer. (b) As in (a) but for linker molecules with a dipole pointing in the opposite direction. (c) Energy-band diagram showing a downward shift of the energy levels of the wide-bandgap nanostructure due to the dipole moment. (d) As in (c) but with linker molecules with a dipole moment pointing away from the QDs (Ruhle et al., 2010).

absorption of the long wavelength light in the solar spectrum, thus enhance the performance of solar cells (Shalav et al., 2005).

Recently, our group has developed 980-nm laser-driven photovoltaic cells (980LD-PVCs) firstly by introducing of a film of rare earth up-converting nanophosphors in conventional dye-sensitized solar cells. The novel photovoltaic cells were constructed by coating Na(Y<sub>1.5</sub>Na<sub>0.5</sub>)F<sub>6</sub>:Yb,Er nanorod films on N3 dye-sensitized TiO<sub>2</sub> films to create direct-current electricity under the irradiation of a 980-nm laser. Under the irradiation of a 980-nm laser with a power of 1 W, the visible up-converting luminescence of rare-earth nanophosphors could be efficiently absorbed by the dyes in 980LD-PVCs, and they exhibited a maximal output power of 0.47 mW. Because of the rather high transparency of biological tissue to 980-nm light, 980LD-PVCs efficiently provided electricity output even when covered by intestinal layers, which promises a new strategy to supply the electrical power for in-vivo nanorobots and other nanobiodevices (Chen et al., 2009).

## 6. Conclusion

DSCs have currently been attracting widespread scientific and technological interest as an alternative to conventional solar cells. The development and future of DSCs are seriously dependent on the optimal combination of high efficiency, good stability, and low cost, which lie on the design, preparation and modification of materials, especially inorganic materials with excellent properties. Nanotechnology opens a door to tailing inorganic materials and creating various nanostructures for the use in DSCs. Currently, inorganic nanomaterials have been widely used in all components. In this chapter, we describe four topics about the application of inorganic nanomaterials in DSCs. Firstly, the preparation and development of semiconductor nanomaterials, including nanoparticles, nanowires and nanotubes for film photoanodes have been demonstrated. Secondly, different nanomaterials, including metal materials, carbon materials and transition-metal compound, have been introduced for the use in photocathodes (counter electrode). Thirdly, the applications of inorganic nanomaterials in quasi-solid/solid-state electrolytes, including *p*-type semiconductor nanoparticles as solid-state electrolytes and solidification of liquid electrolyte by inorganic nanoparticles, have been discussed. At last, the development of semiconductor quantum dots and rare-earth up-converting nanophosphors as light-absorbing material has been presented.

However, these are initial results, and further research is still needed to improve the conversion efficiency and stability of DSCs. In order to further improve the efficiency and facilitate the practical application of DSCs, the following challenges should be addressed: (1) design and preparation transparent nanocrystalline film electrodes with higher surface area and faster electron transport property; (2) development of inorganic nanomaterials with low cost and high catalytic activity as counter electrode materials; (3) preparation of novel quasi-solid/solid-state electrolytes with high thermostability and excellent hole-transporting property; (4) design and construction of semiconductor quantum dots as effective light-absorbing material, especially quantum dots with excellent multiple exciton generation ability; (5) development of new techniques to better control the kinetic electron transfer processes at all interfaces.

## 7. Acknowledgment

This work was financially supported by the National Natural Science Foundation of China (Grant No. 50872020 and 50902021), the Science and Technology Commission of Shanghai-based "Innovation Action Plan" Project (Grant No. 10JC1400100), Shanghai Rising-Star Program (Grant No. 11QA1400100), Shanghai "Chen Guang" project (Grant No. 09CG27), the Fundamental Research Funds for the Central Universities.

## 8. References

- Ardalan, P.; Brennan, T. P.; Lee, H. B. R.; Bakke, J. R.; Ding, I. K.; McGehee, M. D. & Bent, S. F. (2011). Effects of self-assembled monolayers on solid-state cds quantum dot sensitized solar cells. *ACS Nano*, VOL.5, NO.2, pp. 1495-1504.
- Baxter, J. B. & Aydil, E. S. (2005). Nanowire-based dye-sensitized solar cells. *Appl. Phys. Lett.*, VOL.86, NO.5, pp. 053114.
- Beard, M. C.; Knutsen, K. P.; Yu, P. R.; Luther, J. M.; Song, Q.; Metzger, W. K.; Ellingson, R. J. & Nozik, A. J. (2007). Multiple exciton generation in colloidal silicon nanocrystals. *Nano Lett.*, VOL.7, NO.8, pp. 2506-2512.
- Buhbut, S.; Itzhakov, S.; Tauber, E.; Shalom, M.; Hod, I.; Geiger, T.; Garini, Y.; Oron, D. & Zaban, A. (2010). Built-in quantum dot antennas in dye-sensitized solar cells. *ACS Nano*, VOL.4, NO.3, pp. 1293-1298.
- Cao, Y. M.; Bai, Y.; Yu, Q. J.; Cheng, Y. M.; Liu, S.; Shi, D.; Gao, F. F. & Wang, P. (2009). Dye-sensitized solar cells with a high absorptivity ruthenium sensitizer featuring a 2-(hexylthio)thiophene conjugated bipyridine. *J. Phys. Chem. C* VOL.113, NO.15, pp. 6290-6297.
- Chang, J. A.; Rhee, J. H.; Im, S. H.; Lee, Y. H.; Kim, H. J.; Seok, S. I.; Nazeeruddin, M. K. & Gratzel, M. (2010). High-performance nanostructured inorganic-organic heterojunction solar cells. *Nano Lett.*, VOL.10, NO.7, pp. 2609-2612.
- Chapin, D. M.; Fuller, C. S. & Pearson, G. L. (1954). A new silicon p-n junction photocell for converting solar radiation into electrical power. *J. Appl. Phys.*, VOL.25, NO.5, pp. 676-677.
- Chen, S. G.; Chappel, S.; Diamant, Y. & Zaban, A. (2001). Preparation of Nb<sub>2</sub>O<sub>5</sub> coated TiO<sub>2</sub> nanoporous electrodes and their application in dye-sensitized solar cells. *Chem. Mater.*, VOL.13, NO.12, pp. 4629-4634.



- Chen, Z. G.; Chen, H. L.; Hu, H.; Yu, M. X.; Li, F. Y.; Zhang, Q.; Zhou, Z. G.; Yi, T. & Huang, C. H. (2008). Versatile synthesis strategy for carboxylic acid-functionalized upconverting nanophosphors as biological labels. *J. Am. Chem. Soc.*, VOL.130, NO.10, pp. 3023-3029.
- Chen, Z. G.; Li, F. Y. & Huang, C. H. (2007a). Organic d- $\Pi$ -a dyes for dye-sensitized solar cell. *Curr. Org. Chem.*, VOL.11, pp. 1241-1258.
- Chen, Z. G.; Yang, H.; Li, X. H.; Li, F. Y.; Yi, T. & Huang, C. H. (2007b). Thermostable succinonitrile-based gel electrolyte for efficient, long-life dye-sensitized solar cells. *J. Mater. Chem.*, VOL.17, NO.16, pp. 1602-1607.
- Chen, Z. G.; Zhang, L. S.; Sun, Y. G.; Hu, J. Q. & Wang, D. Y. (2009). 980-nm laser-driven photovoltaic cells based on rare-earth up-converting phosphors for biomedical applications. *Adv. Funct. Mater.*, VOL.19, NO.23, pp. 3815-3820.
- Desilvestro, J.; Gratzel, M.; Kavan, L.; Moser, J. & Augustynski, J. (1985). Highly efficient sensitization of titanium-dioxide. *J. Am. Chem. Soc.*, VOL.107, NO.10, pp. 2988-2990.
- Diamant, Y.; Chen, S. G.; Melamed, O. & Zaban, A. (2003). Core-shell nanoporous electrode for dye sensitized solar cells: the effect of the SrTiO<sub>3</sub> shell on the electronic properties of the TiO<sub>2</sub> core. *J. Phys. Chem. B* VOL.107, NO.9, pp. 1977-1981.
- Diguna, L. J.; Shen, Q.; Kobayashi, J. & Toyoda, T. (2007). High efficiency of CdSe quantum-dot-sensitized TiO<sub>2</sub> inverse opal solar cells. *Appl. Phys. Lett.*, VOL.91, NO.2, pp.
- Ellingson, R. J.; Beard, M. C.; Johnson, J. C.; Yu, P. R.; Micic, O. I.; Nozik, A. J.; Shabaev, A. & Efros, A. L. (2005). Highly efficient multiple exciton generation in colloidal PbSe and PbS quantum dots. *Nano Lett.*, VOL.5, NO.5, pp. 865-871.
- Feng, X. J.; Shankar, K.; Varghese, O. K.; Paulose, M.; Latempa, T. J. & Grimes, C. A. (2008). Vertically aligned single crystal TiO<sub>2</sub> nanowire arrays grown directly on transparent conducting oxide coated glass: synthesis details and applications. *Nano Lett.*, VOL.8, NO.11, pp. 3781-3786.
- Frederick, M. T. & Weiss, E. A. (2010). Relaxation of exciton confinement in CdSe quantum dots by modification with a conjugated dithiocarbamate ligand. *ACS Nano*, VOL.4, NO.6, pp. 3195-3200.
- Garcia, C. G.; de Lima, J. F. & Iha, N. Y. M. (2000). Energy conversion: from the ligand field photochemistry to solar cells. *Coord. Chem. Rev.*, VOL.196, pp. 219-247.
- Gimenez, S.; Mora-Sero, I.; Macor, L.; Guijarro, N.; Lana-Villarreal, T.; Gomez, R.; Diguna, L. J.; Shen, Q.; Toyoda, T. & Bisquert, J. (2009). Improving the performance of colloidal quantum-dot-sensitized solar cells. *Nanotechnology*, VOL.20, NO.29, pp. 295204.
- Gonzalez-Pedro, V.; Xu, X. Q.; Mora-Sero, I. & Bisquert, J. (2010). Modeling high-efficiency quantum dot sensitized solar cells. *ACS Nano*, VOL.4, NO.10, pp. 5783-5790.
- Gratzel, M. (2004). Conversion of sunlight to electric power by nanocrystalline dye-sensitized solar cells. *Journal of Photochemistry and Photobiology a-Chemistry*, VOL.164, NO.1-3, pp. 3-14.
- Gratzel, M. (2001). Photoelectrochemical cells. *Nature*, VOL.414, NO.6861, pp. 338-344.
- Gregg, B. A.; Pichot, F.; Ferrere, S. & Fields, C. L. (2001). Interfacial recombination processes in dye-sensitized solar cells and methods to passivate the interfaces. *J. Phys. Chem. B* VOL.105, NO.7, pp. 1422-1429.
- Hagfeldt, A.; Boschloo, G.; Sun, L. C.; Kloo, L. & Pettersson, H. (2010). Dye-sensitized solar cells. *Chem. Rev.*, VOL.110, NO.11, pp. 6595-6663.

- Han, J. B.; Fan, F. R.; Xu, C.; Lin, S. S.; Wei, M.; Duan, X. & Wang, Z. L. (2010). ZnO nanotube-based dye-sensitized solar cell and its application in self-powered devices. *Nanotechnology*, VOL.21, NO.40, pp. 405203.
- Hauch, A. & Georg, A. (2001). Diffusion in the electrolyte and charge-transfer reaction at the platinum electrode in dye-sensitized solar cells. *Electrochim. Acta* VOL.46, NO.22, pp. 3457-3466.
- Heer, S.; Kompe, K.; Gudel, H. U. & Haase, M. (2004). Highly efficient multicolour upconversion emission in transparent colloids of lanthanide-doped NaYF<sub>4</sub> nanocrystals. *Adv. Mater.*, VOL.16, NO.23-24, pp. 2102-2105.
- Hodes, G. (2008). Comparison of dye- and semiconductor-sensitized porous nanocrystalline liquid junction solar cells. *J. Phys. Chem. C* VOL.112, NO.46, pp. 17778-17787.
- Hore, S.; Palomares, E.; Smit, H.; Bakker, N. J.; Comte, P.; Liska, P.; Thampi, K. R.; Kroon, J. M.; Hinsch, A. & Durrant, J. R. (2005). Acid versus base peptization of mesoporous nanocrystalline TiO<sub>2</sub> films: functional studies in dye sensitized solar cellst. *J. Mater. Chem.*, VOL.15, NO.3, pp. 412-418.
- Huang, Z.; Liu, X. H.; Li, K. X.; Li, D. M.; Luo, Y. H.; Li, H.; Song, W. B.; Chen, L. Q. & Meng, Q. B. (2007). Application of carbon materials as counter electrodes of dye-sensitized solar cells. *Electrochem. Commun.*, VOL.9, NO.4, pp. 596-598.
- Hyun, B. R.; Zhong, Y. W.; Bartnik, A. C.; Sun, L. F.; Abruna, H. D.; Wise, F. W.; Goodreau, J. D.; Matthews, J. R.; Leslie, T. M. & Borrelli, N. F. (2008). Electron injection from colloidal PbS quantum dots into titanium dioxide nanoparticles. *ACS Nano*, VOL.2, NO.11, pp. 2206-2212.
- Imoto, K.; Takahashi, K.; Yamaguchi, T.; Komura, T.; Nakamura, J. & Murata, K. (2003). High-performance carbon counter electrode for dye-sensitized solar cells. *Sol. Energy Mater. Sol. Cells* VOL.79, NO.4, pp. 459-469.
- Jiang, Q. W.; Li, G. R. & Gao, X. P. (2009). Highly ordered TiN nanotube arrays as counter electrodes for dye-sensitized solar cells. *Chem. Commun.*, NO.44, pp. 6720-6722.
- Jiang, Q. W.; Li, G. R.; Liu, S. & Gao, X. P. (2010). Surface-nitrided nickel with bifunctional structure as low-cost counter electrode for dye-sensitized solar cells. *J. Phys. Chem. C* VOL.114, NO.31, pp. 13397-13401.
- Joshi, P.; Zhang, L. F.; Chen, Q. L.; Galipeau, D.; Fong, H. & Qiao, Q. Q. (2010). Electrospun carbon nanofibers as low-cost counter electrode for dye-sensitized solar cells. *ACS Appl. Mater. Interfaces* VOL.2, NO.12, pp. 3572-3577.
- Jung, H. S.; Lee, J. K.; Nastasi, M.; Lee, S. W.; Kim, J. Y.; Park, J. S.; Hong, K. S. & Shin, H. (2005). Preparation of nanoporous MgO-Coated TiO<sub>2</sub> nanoparticles and their application to the electrode of dye-sensitized solar cells. *Langmuir*, VOL.21, NO.23, pp. 10332-10335.
- Kaiser, I.; Ernst, K.; Fischer, C. H.; Konenkamp, R.; Rost, C.; Sieber, I. & Lux-Steiner, M. C. (2001). The eta-solar cell with CuInS<sub>2</sub>: A photovoltaic cell concept using an extremely thin absorber (eta). *Sol. Energy Mater. Sol. Cells* VOL.67, NO.1-4, pp. 89-96.
- Kamat, P. V. (2008). Quantum dot solar cells. Semiconductor nanocrystals as light harvesters. *J. Phys. Chem. C* VOL.112, NO.48, pp. 18737-18753.
- Kang, T. S.; Smith, A. P.; Taylor, B. E. & Durstock, M. F. (2009). Fabrication of highly-ordered TiO<sub>2</sub> nanotube arrays and their use in dye-sensitized solar cells. *Nano Lett.*, VOL.9, NO.2, pp. 601-606.

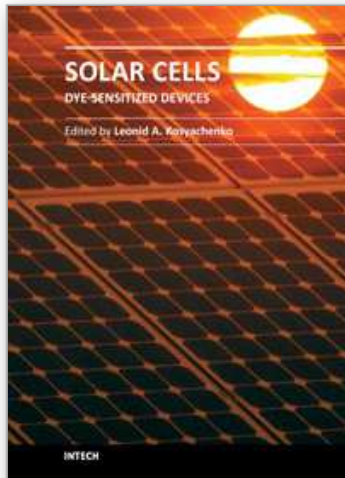
- Kavan, L.; Yum, J. H. & Gratzel, M. (2011). Optically transparent cathode for dye-sensitized solar cells based on graphene nanoplatelets. *ACS Nano*, VOL.5, NO.1, pp. 165-172.
- Kay, A. & Gratzel, M. (1996). Low cost photovoltaic modules based on dye sensitized nanocrystalline titanium dioxide and carbon powder. *Sol. Energy Mater. Sol. Cells* VOL.44, NO.1, pp. 99-117.
- Kay, A. & Gratzel, M. (2002). Dye-sensitized core-shell nanocrystals: Improved efficiency of mesoporous tin oxide electrodes coated with a thin layer of an insulating oxide. *Chem. Mater.* , VOL.14, NO.7, pp. 2930-2935.
- Klimov, V. I. (2006). Mechanisms for photogeneration and recombination of multiexcitons in semiconductor nanocrystals: Implications for lasing and solar energy conversion. *J. Phys. Chem. B* VOL.110, NO.34, pp. 16827-16845.
- Kron, G.; Egerter, T.; Werner, J. H. & Rau, U. (2003). Electronic transport in dye-sensitized nanoporous TiO<sub>2</sub> solar cells-comparison of electrolyte and solid-state devices. *J. Phys. Chem. B* VOL.107, NO.15, pp. 3556-3564.
- Kumara, G. R. A.; Kaneko, S.; Okuya, M. & Tennakone, K. (2002). Fabrication of dye-sensitized solar cells using triethylamine hydrothiocyanate as a CuI crystal growth inhibitor. *Langmuir*, VOL.18, NO.26, pp. 10493-10495.
- Law, M.; Greene, L. E.; Johnson, J. C.; Saykally, R. & Yang, P. D. (2005). Nanowire dye-sensitized solar cells. *Nat. Mater.* , VOL.4, NO.6, pp. 455-459.
- Lee, H.; Leventis, H. C.; Moon, S. J.; Chen, P.; Ito, S.; Haque, S. A.; Torres, T.; Nuesch, F.; Geiger, T.; Zakeeruddin, S. M.; Gratzel, M. & Nazeeruddin, M. K. (2009a). PbS and US quantum dot-sensitized solid-state solar cells: "old concepts, new results". *Adv. Funct. Mater.* , VOL.19, NO.17, pp. 2735-2742.
- Lee, H.; Wang, M. K.; Chen, P.; Gamelin, D. R.; Zakeeruddin, S. M.; Gratzel, M. & Nazeeruddin, M. K. (2009b). Efficient CdSe quantum dot-sensitized solar cells prepared by an improved successive ionic layer adsorption and reaction process. *Nano Lett.* , VOL.9, NO.12, pp. 4221-4227.
- Lee, Y. L. & Lo, Y. S. (2009). Highly efficient quantum-dot-sensitized solar cell based on co-sensitization of CdS/CdSe. *Adv. Funct. Mater.* , VOL.19, NO.4, pp. 604-609.
- Leschkies, K. S.; Jacobs, A. G.; Norris, D. J. & Aydil, E. S. (2009). Nanowire-quantum-dot solar cells and the influence of nanowire length on the charge collection efficiency. *Appl. Phys. Lett.* , VOL.95, NO.19, pp. 193103.
- Levy-Clement, C.; Tena-Zaera, R.; Ryan, M. A.; Katty, A. & Hodes, G. (2005). CdSe-Sensitized p-CuSCN/nanowire n-ZnO heterojunctions. *Adv. Mater.* , VOL.17, NO.12, pp. 1512-1515.
- Lin, S.-C.; Lee, Y.-L.; Chang, C.-H.; Shen, Y.-J. & Yang, Y.-M. (2007). Quantum-dot-sensitized solar cells: Assembly of CdS-quantum-dots coupling techniques of self-assembled monolayer and chemical bath deposition. *Appl. Phys. Lett.* , VOL.90, NO.14, pp. 143517.
- Liu, B. & Aydil, E. S. (2009). Growth of oriented single-crystalline rutile TiO<sub>2</sub> nanorods on transparent conducting substrates for dye-sensitized solar cells. *J. Am. Chem. Soc.* , VOL.131, NO.11, pp. 3985-3990.
- Liu, Y.-X.; Summers, M. A.; Scully, S. R. & McGehee, M. D. (2006). Resonance energy transfer from organic chromophores to fullerene molecules. *J. Appl. Phys.* , VOL.99, NO.9, pp. 093521.

- Lu, S. & Madhukar, A. (2007). Nonradiative resonant excitation transfer from nanocrystal quantum dots to adjacent quantum channels. *Nano Lett.* , VOL.7, NO.11, pp. 3443-3451.
- Macak, J. M.; Tsuchiya, H.; Ghicov, A. & Schmuki, P. (2005). Dye-sensitized anodic TiO<sub>2</sub> nanotubes. *Electrochem. Commun.* , VOL.7, NO.11, pp. 1133-1137.
- Martinson, A. B. F.; Elam, J. W.; Hupp, J. T. & Pellin, M. J. (2007). ZnO nanotube based dye-sensitized solar cells. *Nano Lett.* , VOL.7, NO.8, pp. 2183-2187.
- Matsumura, M.; Matsudaira, S.; Tsubomura, H.; Takata, M. & Yanagida, H. (1980). Dye sensitization and surface structures of semiconductor electrodes. *Ind. Eng. Chem. Prod. Res. Dev.* , VOL.19, NO.3, pp. 415-421.
- Meng, Q. B.; Takahashi, K.; Zhang, X. T.; Sutanto, I.; Rao, T. N.; Sato, O.; Fujishima, A.; Watanabe, H.; Nakamori, T. & Uragami, M. (2003). Fabrication of an efficient solid-state dye-sensitized solar cell. *Langmuir*, VOL.19, NO.9, pp. 3572-3574.
- Muniz, E. C.; Goes, M. S.; Silva, J. J.; Varela, J. A.; Joanni, E.; Parra, R. & Bueno, P. R. (2011). Synthesis and characterization of mesoporous TiO<sub>2</sub> nanostructured films prepared by a modified sol-gel method for application in dye solar cells. *Ceram. Int.* , VOL.37, NO.3, pp. 1017-1024.
- Murakami, T. N.; Kijitori, Y.; Kawashima, N. & Miyasaka, T. (2004). Low temperature preparation of mesoporous TiO<sub>2</sub> films for efficient dye-sensitized photoelectrode by chemical vapor deposition combined with UV light irradiation. *Journal of Photochemistry and Photobiology a-Chemistry*, VOL.164, NO.1-3, pp. 187-191.
- Murray, C. B.; Norris, D. J. & Bawendi, M. G. (1993). Synthesis and characterization of nearly monodisperse CdE (E = S, Se, Te) semiconductor nanocrystallites. *J. Am. Chem. Soc.* , VOL.115, NO.19, pp. 8706-8715.
- Neale, N. R. & Frank, A. J. (2007). Size and shape control of nanocrystallites in mesoporous TiO<sub>2</sub> films. *J. Mater. Chem.* , VOL.17, NO.30, pp. 3216-3221.
- Norris, D. J. & Bawendi, M. G. (1996). Measurement and assignment of the size-dependent optical spectrum in CdSe quantum dots. *Physical Review B*, VOL.53, NO.24, pp. 16338-16346.
- O'Regan, B. & Schwartz, D. T. (1998). Large enhancement in photocurrent efficiency caused by UV illumination of the dye-sensitized heterojunction TiO<sub>2</sub>/RuLL ' NCS/CuSCN: Initiation and potential mechanisms. *Chem. Mater.* , VOL.10, NO.6, pp. 1501-1509.
- O'Regan, B.; Schwartz, D. T.; Zakeeruddin, S. M. & Gratzel, M. (2000). Electrodeposited nanocomposite n-p heterojunctions for solid-state dye-sensitized photovoltaics. *Adv. Mater.* , VOL.12, NO.17, pp. 1263-1267.
- O'Regan, B.; Scully, S.; Mayer, A. C.; Palomares, E. & Durrant, J. (2005). The effect of Al<sub>2</sub>O<sub>3</sub> barrier layers in TiO<sub>2</sub>/Dye/CuSCN photovoltaic cells explored by recombination and DOS characterization using transient photovoltage measurements. *J. Phys. Chem. B* VOL.109, NO.10, pp. 4616-4623.
- O'Regan, B. & Gratzel, M. (1991). A low-cost, high-efficiency solar-cell based on dye-sensitized colloidal TiO<sub>2</sub> films. *Nature*, VOL.353, NO.6346, pp. 737-740.
- O'Regan, B. & Schwartz, D. T. (1995). Efficient photo-hole injection from adsorbed cyanine dyes into electrodeposited copper(I) thiocyanate thin-films. *Chem. Mater.* , VOL.7, NO.7, pp. 1349-1354.
- Overbeek, J. T. G. (1982). Monodisperse colloidal systems, fascinating and useful. *Adv. Colloid Interface Sci.* , VOL.15, NO.3-4, pp. 251-277.

- Park, N. G.; van de Lagemaat, J. & Frank, A. J. (2000). Comparison of dye-sensitized rutile- and anatase-based TiO<sub>2</sub> solar cells. *J. Phys. Chem. B* VOL.104, NO.38, pp. 8989-8994.
- Peng, Z. A. & Peng, X. G. (2002). Nearly monodisperse and shape-controlled CdSe nanocrystals via alternative routes: Nucleation and growth. *J. Am. Chem. Soc.* , VOL.124, NO.13, pp. 3343-3353.
- Ramasamy, E.; Lee, W. J.; Lee, D. Y. & Song, J. S. (2007). Nanocarbon counterelectrode for dye sensitized solar cells. *Appl. Phys. Lett.* , VOL.90, NO.17, pp.
- Robel, I.; Kuno, M. & Kamat, P. V. (2007). Size-dependent electron injection from excited CdSe quantum dots into TiO<sub>2</sub> nanoparticles. *J. Am. Chem. Soc.* , VOL.129, NO.14, pp. 4136-4137.
- Robel, I.; Subramanian, V.; Kuno, M. & Kamat, P. V. (2006). Quantum dot solar cells. Harvesting light energy with CdSe nanocrystals molecularly linked to mesoscopic TiO<sub>2</sub> films. *J. Am. Chem. Soc.* , VOL.128, NO.7, pp. 2385-2393.
- Ross, R. T. & Nozik, A. J. (1982). Efficiency of hot-carrier solar energy converters. *J. Appl. Phys.* , VOL.53, NO.5, pp. 3813-3818.
- Roy-Mayhew, J. D.; Bozym, D. J.; Punckt, C. & Aksay, I. A. (2010). Functionalized graphene as a catalytic counter electrode in dye-sensitized solar cells. *ACS Nano*, VOL.4, NO.10, pp. 6203-6211.
- Roy, P.; Kim, D.; Paramasivam, I. & Schmuki, P. (2009). Improved efficiency of TiO<sub>2</sub> nanotubes in dye sensitized solar cells by decoration with TiO<sub>2</sub> nanoparticles. *Electrochem. Commun.* , VOL.11, NO.5, pp. 1001-1004.
- Ruhle, S.; Shalom, M. & Zaban, A. (2010). Quantum-dot-sensitized solar cells. *ChemPhysChem* VOL.11, NO.11, pp. 2290-2304.
- Sayer, R. A.; Hodson, S. L. & Fisher, T. S. (2010). Improved efficiency of dye-sensitized solar cells using a vertically aligned carbon nanotube counter electrode. *Journal of Solar Energy Engineering-Transactions of the Asme*, VOL.132, NO.2, pp. 021007.
- Schaller, R. D.; Sykora, M.; Pietryga, J. M. & Klimov, V. I. (2006). Seven excitons at a cost of one: Redefining the limits for conversion efficiency of photons into charge carriers. *Nano Lett.* , VOL.6, pp. 424-429.
- Seo, S. H.; Kim, S. Y.; Koo, B. K.; Cha, S. I. & Lee, D. Y. (2010). Influence of electrolyte composition on the photovoltaic performance and stability of dye-sensitized solar cells with multiwalled carbon nanotube catalysts. *Langmuir*, VOL.26, NO.12, pp. 10341-10346.
- Shalav, A.; Richards, B. S.; Trupke, T.; Kramer, K. W. & Gudel, H. U. (2005). Application of NaYF<sub>4</sub>:Er<sup>3+</sup> up-converting phosphors for enhanced near-infrared silicon solar cell response. *Appl. Phys. Lett.* , VOL.86, NO.1, pp. 013505.
- Shankar, K.; Feng, X. & Grimes, C. A. (2009). Enhanced harvesting of red photons in nanowire solar cells: Evidence of resonance energy transfer. *ACS Nano*, VOL.3, NO.4, pp. 788-794.
- Shen, Y.; Bao, J.; Dai, N.; Wu, J.; Gu, F.; Tao, J. C. & Zhang, J. C. (2009). Speedy photoelectric exchange of CdSe quantum dots/mesoporous titania composite system. *Appl. Surf. Sci.* , VOL.255, NO.6, pp. 3908-3911.
- Shi, C.; Zhu, A. M.; Yang, X. F. & Au, C. T. (2004). On the catalytic nature of VN, Mo<sub>2</sub>N, and W<sub>2</sub>N nitrides for NO reduction with hydrogen. *Applied Catalysis a-General*, VOL.276, NO.1-2, pp. 223-230.

- Smestad, G. P.; Spiekermann, S.; Kowalik, J.; Grant, C. D.; Schwartzberg, A. M.; Zhang, J.; Tolbert, L. M. & Moons, E. (2003). A technique to compare polythiophene solid-state dye sensitized TiO<sub>2</sub> solar cells to liquid junction devices. *Sol. Energy Mater. Sol. Cells* VOL.76, NO.1, pp. 85-105.
- Sung, Y. M. & Kim, H. J. (2007). Sputter deposition and surface treatment of TiO<sub>2</sub> films for dye-sensitized solar cells using reactive RF plasma. *Thin Solid Films* VOL.515, NO.12, pp. 4996-4999.
- Suzuki, K.; Yamaguchi, M.; Kumagai, M. & Yanagida, S. (2003). Application of carbon nanotubes to counter electrodes of dye-sensitized solar cells. *Chem. Lett.* , VOL.32, NO.1, pp. 28-29.
- Talapin, D. V. & Murray, C. B. (2005). PbSe nanocrystal solids for n- and p-channel thin film field-effect transistors. *Science*, VOL.310, NO.5745, pp. 86-89.
- Talapin, D. V.; Rogach, A. L.; Shevchenko, E. V.; Kornowski, A.; Haase, M. & Weller, H. (2002). Dynamic distribution of growth rates within the ensembles of colloidal II-VI and III-V semiconductor nanocrystals as a factor governing their photoluminescence efficiency. *J. Am. Chem. Soc.* , VOL.124, NO.20, pp. 5782-5790.
- Tang, Y. W.; Luo, L. J.; Chen, Z. G.; Jiang, Y.; Li, B. H.; Jia, Z. Y. & Xu, L. (2007). Electrodeposition of ZnO nanotube arrays on TCO glass substrates. *Electrochem. Commun.* , VOL.9, NO.2, pp. 289-292.
- Tennakone, K.; Kumara, G.; Kottegoda, I. R. M.; Wijayantha, K. G. U. & Perera, V. P. S. (1998). A solid-state photovoltaic cell sensitized with a ruthenium bipyridyl complex. *Journal of Physics D-Applied Physics*, VOL.31, NO.12, pp. 1492-1496.
- Tennakone, K.; Kumara, G.; Kumarasinghe, A. R.; Wijayantha, K. G. U. & Sirimanne, P. M. (1995). A dye-sensitized nano-porous solid-state photovoltaic cell. *Semicond. Sci. Technol.* , VOL.10, NO.12, pp. 1689-1693.
- Terauchi, S.; Koshizaki, N. & Umehara, H. (1995). Fabrication of Au nanoparticles by radio-frequency magnetron sputtering. *Nanostruct. Mater.* , VOL.5, NO.1, pp. 71-78.
- Tributsch, H. (1972). Reaction of excited chlorophyll molecules at electrodes and in photosynthesis. *Photochem. Photobiol.* , VOL.16, NO.4, pp. 261-269.
- Tributsch, H. (2004). Dye sensitization solar cells: a critical assessment of the learning curve. *Coord. Chem. Rev.* , VOL.248, NO.13-14, pp. 1511-1530.
- Tsubomura, H.; Matsumura, M.; Nomura, Y. & Amamiya, T. (1976). Dye sensitised zinc oxide: aqueous electrolyte: platinum photocell. *Nature*, VOL.261, NO.5559, pp. 402-403.
- Vogel, R.; Hoyer, P. & Weller, H. (1994). Quantum-sized PbS, CdS, Ag<sub>2</sub>S, Sb<sub>2</sub>S<sub>3</sub>, and Bi<sub>2</sub>S<sub>3</sub> particles as sensitizers for various nanoporous wide-bandgap semiconductors. *J. Phys. Chem.* , VOL.98, NO.12, pp. 3183-3188.
- Wang, G. Q.; Xing, W. & Zhuo, S. P. (2009a). Application of mesoporous carbon to counter electrode for dye-sensitized solar cells. *J. Power Sources* VOL.194, NO.1, pp. 568-573.
- Wang, M. K.; Anghel, A. M.; Marsan, B.; Ha, N. L. C.; Pootrakulchote, N.; Zakeeruddin, S. M. & Gratzel, M. (2009b). CoS supersedes Pt as efficient electrocatalyst for triiodide reduction in dye-sensitized solar cells. *J. Am. Chem. Soc.* , VOL.131, NO.44, pp. 15976-15977.
- Wang, P.; Dai, Q.; Zakeeruddin, S. M.; Forsyth, M.; MacFarlane, D. R. & Gratzel, M. (2004). Ambient temperature plastic crystal electrolyte for efficient, all-solid-state dye-sensitized solar CeN. *J. Am. Chem. Soc.* , VOL.126, NO.42, pp. 13590-13591.

- Wang, P.; Zakeeruddin, S. M.; Comte, P.; Exnar, I. & Gratzel, M. (2003a). Gelation of ionic liquid-based electrolytes with silica nanoparticles for quasi-solid-state dye-sensitized solar cells. *J. Am. Chem. Soc.*, VOL.125, NO.5, pp. 1166-1167.
- Wang, P.; Zakeeruddin, S. M.; Moser, J. E.; Nazeeruddin, M. K.; Sekiguchi, T. & Gratzel, M. (2003b). A stable quasi-solid-state dye-sensitized solar cell with an amphiphilic ruthenium sensitizer and polymer gel electrolyte. *Nat. Mater.*, VOL.2, NO.6, pp. 402-407.
- Wang, Z.-S.; Yanagida, M.; Sayama, K. & Sugihara, H. (2006). Electronic-insulating coating of CaCO<sub>3</sub> on TiO<sub>2</sub> electrode in dye-sensitized solar cells: Improvement of electron lifetime and efficiency. *Chem. Mater.*, VOL.18, NO.12, pp. 2912-2916.
- Wang, Z. S.; Huang, C. H.; Huang, Y. Y.; Hou, Y. J.; Xie, P. H.; Zhang, B. W. & Cheng, H. M. (2001). A highly efficient solar cell made from a dye-modified ZnO-covered TiO<sub>2</sub> nanoporous electrode. *Chem. Mater.*, VOL.13, NO.2, pp. 678-682.
- Wroblowa, H. S. & Saunders, A. (1973). Flow-through electrodes: II. The I<sub>3</sub><sup>-</sup>/I<sup>-</sup> redox couple. *J. Electroanal. Chem. Interfacial Electrochem.*, VOL.42, NO.3, pp. 329-346.
- Wu, M.; Lin, X.; Hagfeldt, A. & Ma, T. (2011a). Low-cost molybdenum carbide and tungsten carbide counter electrodes for dye-sensitized solar cells. *Angew. Chem. Int. Ed.*, VOL.50, NO.15, pp. 3520-3524.
- Wu, M. X.; Lin, X. A.; Hagfeldt, A. & Ma, T. L. (2011b). A novel catalyst of WO<sub>2</sub> nanorod for the counter electrode of dye-sensitized solar cells. *Chem. Commun.*, VOL.47, NO.15, pp. 4535-4537.
- Wu, S. J.; Han, H. W.; Tai, Q. D.; Zhang, J.; Chen, B. L.; Xu, S.; Zhou, C. H.; Yang, Y.; Hu, H. & Zhao, X. Z. (2008). Improvement in dye-sensitized solar cells with a ZnO-coated TiO<sub>2</sub> electrode by rf magnetron sputtering. *Appl. Phys. Lett.*, VOL.92, NO.12, pp. 122106.
- Xia, J. B.; Li, F. Y.; Yang, H.; Li, X. H. & Huang, C. H. (2007). A novel quasi-solid-state dye-sensitized solar cell based on monolayer capped nanoparticles framework materials. *Journal of Materials Science*, VOL.42, NO.15, pp. 6412-6416.
- Yang, H.; Cheng, Y. F.; Li, F. Y.; Zhou, Z. G.; Yi, T.; Huang, C. H. & Jia, N. Q. (2005). Quasi-solid-state dye-sensitized solar cells based on mesoporous silica SBA-15 framework materials. *Chin. Phys. Lett.*, VOL.22, NO.8, pp. 2116-2118.
- Yoon, C. H.; Vittal, R.; Lee, J.; Chae, W. S. & Kim, K. J. (2008). Enhanced performance of a dye-sensitized solar cell with an electrodeposited-platinum counter electrode. *Electrochim. Acta* VOL.53, NO.6, pp. 2890-2896.
- Zaban, A.; Aruna, S. T.; Tirosh, S.; Gregg, B. A. & Mastai, Y. (2000). The effect of the preparation condition of TiO<sub>2</sub> colloids on their surface structures. *J. Phys. Chem. B* VOL.104, NO.17, pp. 4130-4133.
- Zhang, Q. F. & Cao, G. Z. (2011). Nanostructured photoelectrodes for dye-sensitized solar cells. *Nano Today*, VOL.6, NO.1, pp. 91-109.
- Zhu, K.; Neale, N. R.; Miedaner, A. & Frank, A. J. (2007). Enhanced charge-collection efficiencies and light scattering in dye-sensitized solar cells using oriented TiO<sub>2</sub> nanotubes arrays. *Nano Lett.*, VOL.7, NO.1, pp. 69-74.



## **Solar Cells - Dye-Sensitized Devices**

Edited by Prof. Leonid A. Kosyachenko

ISBN 978-953-307-735-2

Hard cover, 492 pages

**Publisher** InTech

**Published online** 09, November, 2011

**Published in print edition** November, 2011

The second book of the four-volume edition of "Solar cells" is devoted to dye-sensitized solar cells (DSSCs), which are considered to be extremely promising because they are made of low-cost materials with simple inexpensive manufacturing procedures and can be engineered into flexible sheets. DSSCs are emerged as a truly new class of energy conversion devices, which are representatives of the third generation solar technology. Mechanism of conversion of solar energy into electricity in these devices is quite peculiar. The achieved energy conversion efficiency in DSSCs is low, however, it has improved quickly in the last years. It is believed that DSSCs are still at the start of their development stage and will take a worthy place in the large-scale production for the future.

### **How to reference**

In order to correctly reference this scholarly work, feel free to copy and paste the following:

Zhigang Chen, Qiwei Tian, Minghua Tang and Junqing Hu (2011). The Application of Inorganic Nanomaterials in Dye-Sensitized Solar Cells, *Solar Cells - Dye-Sensitized Devices*, Prof. Leonid A. Kosyachenko (Ed.), ISBN: 978-953-307-735-2, InTech, Available from: <http://www.intechopen.com/books/solar-cells-dye-sensitized-devices/the-application-of-inorganic-nanomaterials-in-dye-sensitized-solar-cells>

**INTECH**  
open science | open minds

### **InTech Europe**

University Campus STeP Ri  
Slavka Krautzeka 83/A  
51000 Rijeka, Croatia  
Phone: +385 (51) 770 447  
Fax: +385 (51) 686 166  
[www.intechopen.com](http://www.intechopen.com)

### **InTech China**

Unit 405, Office Block, Hotel Equatorial Shanghai  
No.65, Yan An Road (West), Shanghai, 200040, China  
中国上海市延安西路65号上海国际贵都大饭店办公楼405单元  
Phone: +86-21-62489820  
Fax: +86-21-62489821



© 2011 The Author(s). Licensee IntechOpen. This is an open access article distributed under the terms of the [Creative Commons Attribution 3.0 License](#), which permits unrestricted use, distribution, and reproduction in any medium, provided the original work is properly cited.

IntechOpen

IntechOpen